Journal of Building Engineering 78 (2023) 107546

Contents lists available at ScienceDirect

Journal of Building Engineering

journal homepage: www.elsevier.com/locate/jobe

Characterization and life cycle assessment of geopolymer mortars with masonry units and recycled concrete aggregates assorted from construction and demolition waste

Anil Kul [a,b], Behlul Furkan Ozel [c], Emircan Ozcelikci [a,b], Muhammed Faruk Gunal [b,d], Huseyin Ulugol [e], Gurkan Yildirim [b,f,*], Mustafa Sahmaran [b]

[a] Hacettepe University, Institute of Science, Beytepe, Ankara, Turkey
[b] Department of Civil Engineering, Hacettepe University, Ankara, Turkey
[c] Department of Civil Engineering, Yozgat Bozok University, Yozgat, Turkey
[d] Ministry of Environment, Urbanization, and Climate Change, Ankara, Turkey
[e] Department of Civil Engineering, Ankara University, Ankara, Turkey
[f] Department of Civil and Structural Engineering, University of Bradford, Bradford, UK

ARTICLE INFO

Keywords:
Geopolymer
Construction and demolition waste (CDW)
Interfacial transition zone
Compressive strength
Life cycle assessment

ABSTRACT

Developing a fast, cost-effective, eco-friendly solution to recycle large amounts of construction and demolition waste (CDW) generated from construction industry-related activities and natural disasters is crucial. The present investigation aims to offer a solution for repurposing CDW into building materials suitable for accelerated construction and housing in developing countries and disaster-prone areas. Feasibility of recycled concrete aggregate (RCA) inclusion in geopolymer mortars constituted entirely from CDW (masonry elements) was investigated via an environmental impact-oriented approach by addressing the composition related key parameters. Mechanical performance was evaluated through compressive strength tests, and scanning electron microscope (SEM) imaging with line mapping analyses were carried out to monitor the interfacial transition zone (ITZ) properties. To investigate the environmental impacts of the geopolymer mortars and highlight the advantages over Portland cement-based mortars, a cradle-to-gate life cycle assessment (LCA) was performed. Findings revealed that roof tile (RT)-based geopolymer mortars mainly exhibited better strength performance due to their finer particle size. Mixtures activated with 15 M NaOH solution and cured at 105 °C achieved an average compressive strength above 55 MPa. RCA size was the most influential parameter on compressive strength, and a smaller maximum RCA size significantly increased the compressive strength. Microstructural analyses showed that the ITZ around smaller RCAs was relatively thinner, resulting in better compressive strength results. LCA proved that CDW-based geopolymer mortars provide the same compressive strength with around 60% less CO_2 emissions and similar energy consumption compared to Portland cement-based mortars.

List of abbreviations

AASC Alkali-Activated Slag Concrete

* Corresponding author. Department of Civil Engineering, Hacettepe University, Ankara, Turkey.
E-mail addresses: g.yildirim@bradford.ac.uk, gurkanyildirim@hacettepe.edu.tr (G. Yildirim).

https://doi.org/10.1016/j.jobe.2023.107546
Received 16 April 2023; Received in revised form 26 May 2023; Accepted 9 August 2023
Available online 9 August 2023

AP	Acidification Potential
CDW	Construction and Demolition Waste
CW	Concrete Waste
EP	Eutrophication Potential
EPA	Environmental Protection Agency
EU	European Union
FA	Fly Ash
FFD	Fossil Fuel Depletion
GGBFS	Ground Granulated Blast Furnace Slag
GHG	Greenhouse Gas
GWP	Global Warming Potential
HB	Hollow Brick
ITZ	Interfacial Transition Zone
LCA	Life Cycle Assessment
LCI	Life Cycle Inventory
LCIA	Life Cycle Impact Assessment
MJ	Megajoule
MSI	Material Sustainability Indicators
NH_x	Nitrogen
NO_x	Nitrous Oxide
ODP	Ozone Depletion Potential
PC	Portland Cement
PCF	Portland Cement-Fly Ash-based Mortar
PDF	Powder Diffraction File
RCA	Recycled Concrete Aggregate
RCB	Red Clay Brick
RT	Roof Tile
SEM	Scanning Electron Microscope
SH	Sodium Hydroxide-NaOH
SO_2	Sulfur Dioxide
SP	Superplasticizer
SS	Sodium Silicate-Na_2SiO_3
UV	Ultraviolet
W	Water
XRD	X-ray Diffraction
XRF	X-ray Fluorescence

1. Introduction

Geopolymeric binders are a promising alternative to reduce carbon emissions from cement production by utilizing industrial by-products as precursors. Compared to Portland cement (PC), geopolymers can significantly decrease CO_2 emissions by 60–90% [1]. Geopolymers belong to the alkali-activated materials family and is a low-calcium variant. It is formed by polymerizing aluminosilicate precursors with the help of alkaline liquids and/or soluble silicates [2]. Geopolymerization is a complex process involving dissolution, orientation, and polycondensation stages, resulting in the formation of a 3D network of silico-aluminate structures [3]. The properties of the end product are influenced by precursor characteristics such as source, composition, and particle size, in addition to alkaline liquid concentration and curing conditions [4]. While fly ash and ground granulated blast furnace slag are commonly used precursors in geopolymer production due to their suitable SiO_2 and Al_2O_3 content, they are no longer considered waste and are widely used as pozzolans in the construction industry [5,6]. Moreover, they have currently been in great demand and can be sold at comparable prices to that of PC. Therefore, current research in geopolymer technology shifts towards utilizing more challenging and locally available waste materials as precursors.

With an annual generation of 820 million tons, construction and demolition waste (CDW) poses a significant environmental challenge, accounting for 46% of total waste in Europe [7]. CDW is typically disposed of in landfills or dumped without recycling, leading to the depletion of valuable land resources and threatening sustainable development [8]. Urgent measures are needed to explore innovative and efficient approaches for recycling and reusing CDW, as its environmental impact can disrupt the ecological balance. Fortunately, components from CDW such as different masonry units with high aluminosilicate content, hold great potential for geopolymerization. Recent studies have demonstrated the feasibility of utilizing ceramic and masonry wastes as precursors in geopolymer production. One of the most recent studies on geopolymers from CDW highlighted that CDW-based roof tiles, red clay bricks, and hollow bricks, which were activated with a 12.5 M NaOH solution and subjected to thermal curing, exhibited compressive strengths around 40 MPa, while glass-based geopolymers under same conditions reached approximately 30 MPa [9]. This was

attributed to the comparatively lower Al_2O_3 content of glass (1.27%) and its relatively coarse particle size distribution compared to the other materials under investigation. Another study focusing on the use of binary combinations of CDW-based masonry elements as precursors rather than single utilization [10] demonstrated that the CDW-based masonry precursors can be combined to manufacture alkali-activated binders, which is likely to eliminate the need for selective demolishment and individual separation. Compressive strength results of these binders were found to increase with higher curing temperatures, longer curing periods, higher NaOH molarity, and increased amounts of hollow brick in the precursor combination. Optimal results were obtained at a curing temperature/period of 115 °C/48 h and NaOH concentration of 15 M, achieving compressive strengths of up to 80 MPa. In another recent study [11], mechanical and durability-related parameters of geopolymer mortars incorporating 100% mixed CDW-based materials as precursors and recycled concrete as fine aggregates with various alkali activator ratios and slag substitutions were investigated. Ambient-cured mortars made solely from CDW-based components (combined masonry, glass and concrete) achieved 30 MPa compressive strength, while slag substituted mixtures reached 50 MPa after 28 days. Slag substitution reduced water absorption, porosity, and drying shrinkage while improving compressive strength. Drying shrinkage had a linear correlation with porosity, and increased shrinkage observed when sodium silicate was used in mixtures' alkali activator combinations. Considering the fact that the diversity in different CDW leads to significant variations in the content of aluminosilicious materials, higher Si/Al ratio enhanced the compressive strength of mixtures by influencing the formation of alkali aluminosilicate gels [12]. Increasing the available silica content in the alkali activated system significantly alters the composition and structure of the gels, resulting in polymerized and densely packed reaction products with improved compressive strength. Moreover, the Ca/Si and Si/Al ratios were clearly impacful parameters on the mechanical performance of the developed mixtures. While researchers have directed their efforts towards investigating CDW-based geopolymeric mixtures, there is a pressing need for comprehensive and inclusive studies to optimize the diverse range of chemical and morphological characteristics of these waste components to utilize all CDW fractions effectively taking their quality and quantity into account.

Concrete waste (CW), which has the largest share among CDW components in most countries [13], is widely used as recycled concrete aggregate (RCA) in practical applications. However, the RCA production is still limited considering that the amount of RCA generated in the EU is only about 9.4% of the total aggregate demand [14]. Parthiban et al. [15], who investigated the influence of RCA on the mechanical and durability properties of ambient-cured alkali-activated slag concrete (AASC) stated that all AASC mixtures exhibited superior mechanical performance than PC-based concrete and the highest strength was achieved with a 50% RCA content. Koushkbaghi et al. [16] found that replacing 30% of RCA in metakaolin geopolymer concrete decreased compressive strength by 28%. Adhesion of old mortar to RCA weakened the aggregate-paste interface, but overlapping hydration products enhanced geopolymer paste formation. In another study, Rahman and Khattak [17], who developed roller-compacted geopolymer concrete using 100% RCA, stated that RCA-based concrete exhibited satisfactory compressive strength (7.53–27.6 MPa), flexural strength (2.1–3.8 MPa), and elastic modulus (15.97–46.77 GPa), making it suitable for robust base pavement. Although the abovementioed studies have shown the feasibility of using RCA in geopolymer-based systems, the potential advantages and shortcomings of including RCA in CDW-based geopolymers are still unclear. In the authors' previous studies [18–20], the RCA was used successfully in CDW-based geopolymer systems, while the effects of aggregate-related properties such as size and amount were not detailed. Additionally, the ITZ properties of RCA used in CDW-based geopolymer matrix have remained unclarified.

Notwithstanding the fact that geopolymers are considered an environmentally friendly alternative to cement given the presence of industrial by-products/wastes in the systems, it is critical to precisely identify their environmental impacts. At this point, the Life Cycle Assessment (LCA) analysis method, a sustainable development tool used to measure and compare the environmental impacts of products and services throughout the entire life cycle, can be lifesaving [21]. In this context, many studies have been conducted to evaluate the environmental effects of geopolymer binders. Geopolymer binders have been reported to cause 27–64% less greenhouse gas emissions compared to conventional cement-based binders [22–27]. However, related assessments are subject to variation because the contents of the examined materials are different and the database, inventory, assumptions, and boundaries employed differ; hence, making a direct comparison may not stand on a sound basis. Although the number of LCA studies for conventional geopolymer systems has reached a certain level, it is very limited for the CDW-based geopolymers. Investigating the energy consumption and CO_2 emissions of the geopolymers produced with the brick-PC combination, Fořt et al. [28], reported that increasing the brick content could reduce the carbon footprints and energy consumption of the mixtures by 63% and 81%, respectively. In addition, the geopolymer mixture (3:7-PC:brick) exhibiting mechanical performance comparable to the completely PC-containing mixture, reduced energy consumption and GHG emissions by 45% and 72%, respectively. A study [29] analyzed the environmental impact of geopolymer mixtures produced from recycled brick and ceramic tile. The results showed that the mixture containing fly ash had the lowest impact on environmental impact categories, including Ozone Depletion Potential (ODP), Global Warming Potential (GWP), Acidification Potential (AP), Eutrophication Potential (EP), and Fossil Fuel Depletion. The use of alkali activators was found to have a greater impact than the manufacturing process. The thermal curing process had a low impact and the highest difference was noted for GWP with about 10 kg. CO_2.eq. In another study [30], the environmental impact of CDW-based Engineered Geopolymer Composites was investigated and the negative effects of alkali activator use were confirmed. However, it was revealed that the optimization of the mixture design and the use of renewable energy resources in the production of alkali activators could bring serious positive results.

It is important to come up with a fast, easy-to-apply, economical, and environmentally friendly solution for the re-utilization and upcycling of the enormous levels of CDW generated as a result of activities related to construction industry and natural disasters such as earthquakes and floods. More specifically, concrete and masonry fractions are critically important as they constitute the largest share of CDW. Moreover, the overview of literature presented above is clear that studies targeting to develop geopolymeric materials based fully on CDW are quite scarce not to mention the in-depth evaluation of environmental impacts of such materials. Current study therefore focuses on the development of heat-cured geopolymer mortars with entirely CDW-based components (*i.e.*, different masonry

units as the geopolymer binder and RCA) with special emphasis on the effects of RCA parameters (size, amount, ITZ properties) and LCA of developed mortars following cradle-to-gate approach to reveal their environmental impacts. Accelerated heat curing was chosen to meet the early strength requirements adequate for the purposes of structural elements especially for the disaster-prone areas and/or countries with fast developing construction and housing industry. Geopolymers and related materials are frequently being reported more advantageous than the traditional cementitious counterparts in terms of environmental considerations. However, quantification of such aspects via detailed LCA analysis is greatly lacking especially in the cases where CDW used both as precursors and aggregates. This is also important for raising the interest and awareness in value-added utilization of CDW through innovative techniques such as geopolymerization.

2. Experimental program

2.1. Materials

2.1.1. CDW-based precursors

CDW-based masonry components including hollow brick (HB), red clay brick (RCB), and roof tile (RT) were collected from an urban transformation area after being categorized and used as precursors in the production of geopolymer mortars. A two-step crushing-grinding process was used to pulverize each CDW-based material. In the first step, materials were crushed and downsized using a laboratory-type jaw crusher with a 1 mm jaw opening. Crushed materials were placed into a laboratory-type mill with steel balls and ground for an hour in the second step. The digital images of the original, ground CDW-based precursors and their SEM images are shown in Fig. 1. The particle size distributions and characteristic particle diameters are demonstrated in Fig. 2 and Table 1, respectively. As seen, at least 90% of all precursors passed through 50 μm, which can be considered satisfactory. According to Komnitsas et al. [31], the mechanical performance of geopolymers can be significantly enhanced using precursors with particle size fractions of 50% that pass through a 15 μm sieve (d(0.5) < 15 μm). Correspondingly, d(0.5) values are 5.39 μm, 8.50 μm, and 4.75 μm for HB, RCB, and RT, respectively. The chemical compositions of CDW-based precursors as determined by X-ray fluorescence (XRF) analysis are presented in Table 2. As discussed earlier, the CDW-based precursors are suitable materials for geopolymerization due to their high SiO_2 and Al_2O_3 contents. Accordingly, the total SiO_2 and Al_2O_3 contents of HB, RCB, and RT are around 70 ± 3%. X-ray diffraction (XRD) analysis of the precursors is displayed in Fig. 3.

The powder diffraction file (PDF) numbers with chemical formulas of crystal phases are also listed in Table 3. The RT, RCB, and HB precursors were semi-crystalline with slight discrepancies and comparable XRD patterns. As expected, apparent quartz peaks were found at 26.5° in all CDW-based precursors. The observed quartz mineral is a tetrahedral structure created between silicon atoms and oxygen that crystallizes in the hexagonal system and has beneficial impacts on the mechanical characteristics of geopolymers due to its ability to provide barriers for crack propagation [32]. Apart from quartz, the major peaks were detected as cristobalite, tridymite, diopside, and lazurite crystals for CDW-based precursors. The tridymite and cristobalite phases are open-structured silica polymorphs that can dissolve twice as fast as quartz in an alkaline environment [33]. These phases arise from the sintering of masonry units at 800–1000 °C, which causes changes in crystalline clay networks [34].

2.1.2. Recycled concrete aggregate

Recycled concrete aggregate (RCA) with unknown properties and finer than 5 mm, was obtained from concrete waste (CW) collected from an urban transformation area. First, CW was crushed with the help of a hammer drill, then fed into a jaw crusher to reduce the particle size. In this stage, jaw opening of the crusher was set to 5 mm, 2 mm, and 1 mm to ensure acquirement of RCA with different sizes. Afterwards, obtained RCA was passed through sieves having 4.75-2.00-0.85-0.10 mm openings, respectively. At last, it was assorted into three different size ranges of 4.75–2.00 mm, 2.00–0.85 mm, and 0.85–0.10 mm. The images and physical properties of RCA are illustrated in Fig. 4 and Table 4, respectively.

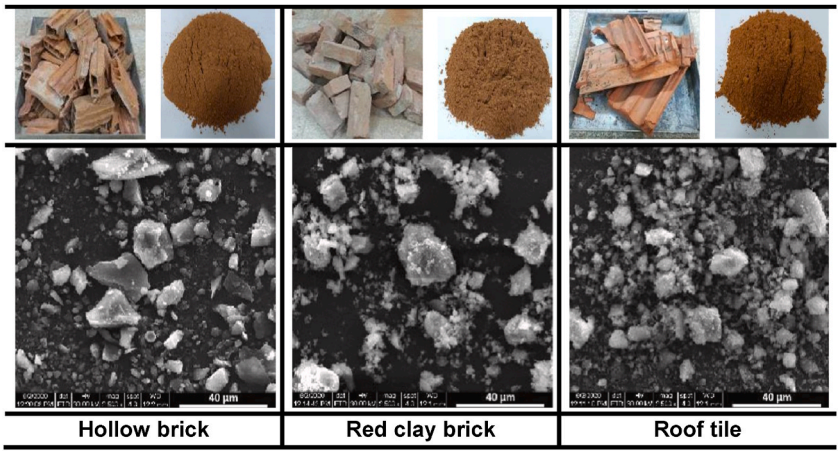

Fig. 1. Original, ground, and SEM views of CDW-based precursors.

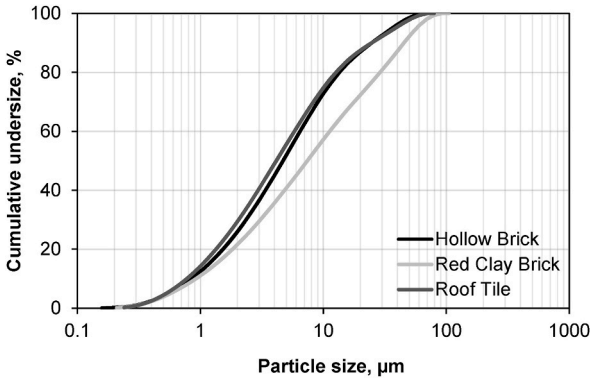

Fig. 2. Particle size distributions of CDW-based precursors.

Table 1
Characteristic particle diameters of CDW-based precursors (units are in μm).

Properties	Hollow brick	Red clay brick	Roof tile
Surface-weighted mean diameter D[3.2]	2.45	2.89	2.32
Volume-weighted mean diameter D[4.3]	10.45	18.00	10.26
d(0.1)	0.97	1.06	0.89
d(0.5)	5.39	8.50	4.75
d(0.9)	28.42	51.85	28.38

Table 2
Chemical compositions of CDW-based precursors.

Chemical composition, %	Hollow brick	Red clay brick	Roof tile
Loss on ignition	4.91	4.68	6.64
SiO_2	53.5	52.4	49.3
Al_2O_3	19.3	19.9	20.0
Fe_2O_3	7.45	7.92	8.16
CaO	4.21	4.18	5.16
MgO	2.61	2.84	3.29
SO_3	1.46	0.95	0.79
Na_2O	1.50	1.58	1.23
K_2O	3.58	3.72	3.67
TiO_2	0.92	1.06	1.08

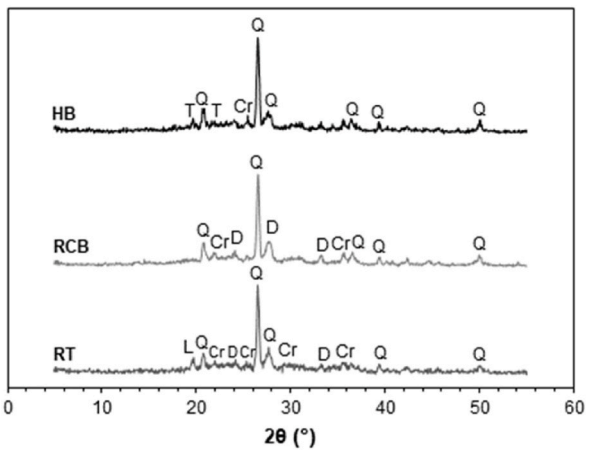

Fig. 3. X-ray diffractograms of CDW-based precursors.

Table 3
Crystalline phases of the precursors as determined by the XRD analyses.

Crystalline phase	Symbol	PDF number	Chemical formula
Quartz	Q	96-901-1494	SiO_2
Cristobalite	Cr	96-900-1581	SiO_2
Tridymite	T	96-901-3394	SiO_2
Diopside	D	96-900-1333	$Al_{0.06}\ Ca_{0.91}\ Fe_{0.1}\ Mg_{0.91}\ Na_{0.05}\ O_6\ Si_{1.97}$
Lazurite	L	96-901-1357	$Al_{2.91}\ Ca_{0.6}\ Na_{3.48}\ O_{11.52}\ Si_{3.09}$

2.1.3. Sodium hydroxide

For an alkali activation, commercially available sodium hydroxide with a minimum of 98% sodium hydroxide, a maximum of 0.4% sodium carbonate, 0.1% sodium chloride, and a maximum of 15 ppm iron was used in a flake form.

2.2. Mixture design

The experimental program included a total of 81 mixtures (27 different combinations for each precursor type), which were prepared based on differences in the precursor type (HB, RCB, and RT), molar concentration of NaOH solution (10 M, 15 M, and 19 M), RCA size (4.75–2.00 mm, 2.00–0.85 mm, 0.85–0.10 mm), and RCA/binder ratio (0.36, 0.45, and 0.55). These mixtures were subjected to different curing temperatures of 105 °C, 115 °C, and 125 °C for 72 h. The mixture proportions are given in Table 5. Following order was used in coding of the mixtures: precursor type-RCA size-NaOH molarity-RCA/binder ratio. For the sake of simplicity, the mixtures were collectively presented under CDW title instead of listing the precursors separately in Table 5. Additionally, RCA sizes were abbreviated for simplicity as 4.75–2.00 mm [A], 2.00–0.85 mm [B], and 0.85–0.10 mm [C]. For instance, HB-C-19-0.55 coded mixture corresponds to hollow brick-based geopolymer mortar containing 0.85–0.10 mm RCA activated with 19 M sodium hydroxide solution and RCA/binder ratio of 0.55.

2.3. Casting, curing, and testing details

The production procedure of mortars began with the preparation of NaOH solutions. NaOH pellets were dissolved in tap water at different concentrations of 10 M, 15 M, and 19 M and allowed to cool in the laboratory until room temperature was attained. In the mixing stage, the CDW-based precursors and RCA were put into a mortar mixer and mixed at 100 rpm for 60 s. Then, NaOH solution was slowly added to the mixture in 30 s, and mixing was continued for further 210 s. At last, the mortar was allowed to mix for an additional 60 s at 150 rpm before the end of mixing. The fresh mortars were cast into pre-oiled cubic molds having 50 mm dimensions and placed immediately into an oven for 72 h to heat cure. The water/binder ratio was kept constant for all mixtures at 0.35. Following the heat curing, mortars were immediately removed and demolded. The views of cubic specimens in the fresh state, after curing, and hardened state are shown in Fig. 5.

The mechanical performance characterization was made through compressive strength test, according to ASTM C109 [35]. Tests were performed by using a 100-ton capacity loading device. Compressive strength results of the mortars were also evaluated by Pearson Correlation to statistically determine which parameter was more effective on strength. The Pearson's correlation coefficient is a tool used to determine what kind of a relationship exists between the two variables. It can have a value between −1 and 1, with −1 indicating a strong inverse relationship, 0 indicating no relationship and 1 indicating a strong direct relationship [36]. Along with the compressive strength test, line mapping analysis via SEM was made to reveal the aggregate, paste, and ITZ structures in mortars containing RCA with different sizes. The process involves scanning a small sample area with an electron beam in a linear pattern, then determining the composition and distribution of elements on the sample's surface.

3. Results and discussion

3.1. Compressive strength

In Fig. 6, the compressive strength results of CDW-based geopolymer mortars are illustrated. The results are presented as the average of six cubic specimens. Strength results ranged between 23.1 and 66.2 MPa with a maximum deviation of ±6 MPa. Additionally, in Table 6, the correlation coefficients of mortar strength for aggregate size, curing temperature.

NaOH molarity, and RCA/binder ratio are provided to evaluate which parameter contributed more to the compressive strength. In parallel, the highest correlation coefficients, the indicators of improved compressive strength, were achieved by RCA size as −0.679, −0.555, and −0.676 for HB, RCB, and RT, respectively. Here, the minus sign indicates an inverse relationship which means the strength increases with the decrease in RCA size. The RCA/binder ratio was the least effective parameter considering the lowest

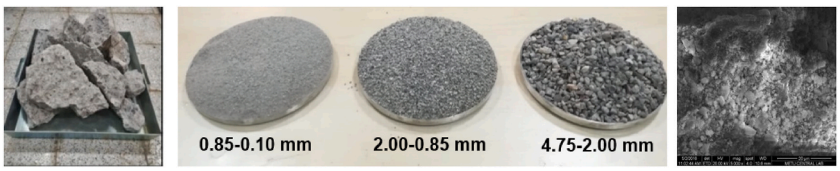

Fig. 4. Digital camera and SEM images of as-obtained and different-size CW.

Table 4
Physical properties of RCA according to particle size ranges.

Properties	4.75–2.00 mm	2.00–0.85 mm	0.85–0.10 mm
Compacted bulk density, kg/m^3	1395.8	1338.9	1346.4
Loose bulk density, kg/m^3	1261.5	1198.2	1251.3
Specific gravity	2.44	2.32	2.11
Water absorption, %	4.07	6.81	13.09
Porosity, %	9.48	14.76	24.42

Table 5
Mixture proportions.

Precursor, 1000gr	Mixture ID.	RCA/binder	RCA, gr	Molarity	NaOH, gr	RCA size, mm
CDW (HB or RCB or RT)	CDW-A-10-0.36	0.36	360	10	139.09	4.75–2.00
	CDW-A-15-0.36			15	208.73	
	CDW-A-19-0.36			19	260.91	
	CDW-A-10-0.45	0.45	450	10	139.09	
	CDW-A-15-0.45			15	208.73	
	CDW-A-19-0.45			19	260.91	
	CDW-A-10-0.55	0.55	550	10	139.09	
	CDW-A-15-0.55			15	208.73	
	CDW-A-19-0.55			19	260.91	
	CDW-B-10-0.36	0.36	360	10	139.09	2.00–0.85
	CDW-B-15-0.36			15	208.73	
	CDW-B-19-0.36			19	260.91	
	CDW-B-10-0.45	0.45	450	10	139.09	
	CDW-B-15-0.45			15	208.73	
	CDW-B-19-0.45			19	260.91	
	CDW-B-10-0.55	0.55	550	10	139.09	
	CDW-B-15-0.55			15	208.73	
	CDW-B-19-0.55			19	260.91	
	CDW-C-10-0.36	0.36	360	10	139.09	0.85–0.10
	CDW-C-15-0.36			15	208.73	
	CDW-C-19-0.36			19	260.91	
	CDW-C-10-0.45	0.45	450	10	139.09	
	CDW-C-15-0.45			15	208.73	
	CDW-C-19-0.45			19	260.91	
	CDW-C-10-0.55	0.55	550	10	139.09	
	CDW-C-15-0.55			15	208.73	
	CDW-C-19-0.55			19	260.91	

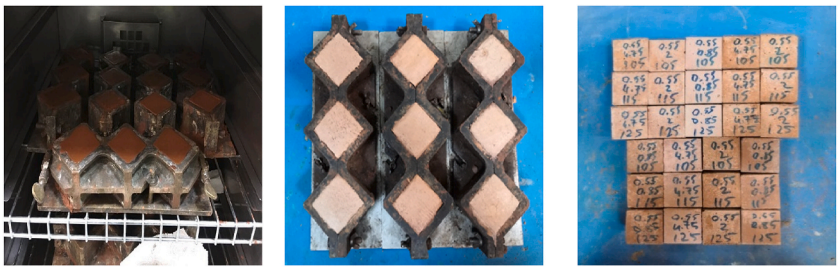

Fig. 5. Views of cubic specimens in the fresh state, after curing, and in the hardened state (left to right).

correlation coefficients. Detailed discussions of the compressive strength results are given in the following sections.

3.1.1. Effect of precursor type

Considering CDW-based precursor types, the RT-based geopolymer mortars achieved the highest average compressive strength, followed by HB- and RCB-based mortars, respectively. Among all mixtures, the maximum compressive strength was 66.2 MPa, achieved by the RT-C-15-0.45 coded mixture. As discussed in earlier sections, compressive strength can be remarkably enhanced when the d(0.5) value is smaller than 15 μm [31]. Accordingly, d(0.5) values of precursors were 5.39 μm, 8.50 μm, and 4.75 μm for HB, RCB, and RT, respectively. Finer particles may have better reactivity and stronger geopolymerization, leading to a denser microstructure. This is primarily due to the increased specific surface area, which increases the reaction rate since the dissolution phase proceeds faster, resulting in an accelerated setting and rapid strength development [6]. Another key parameter affecting the strength is the precursors'

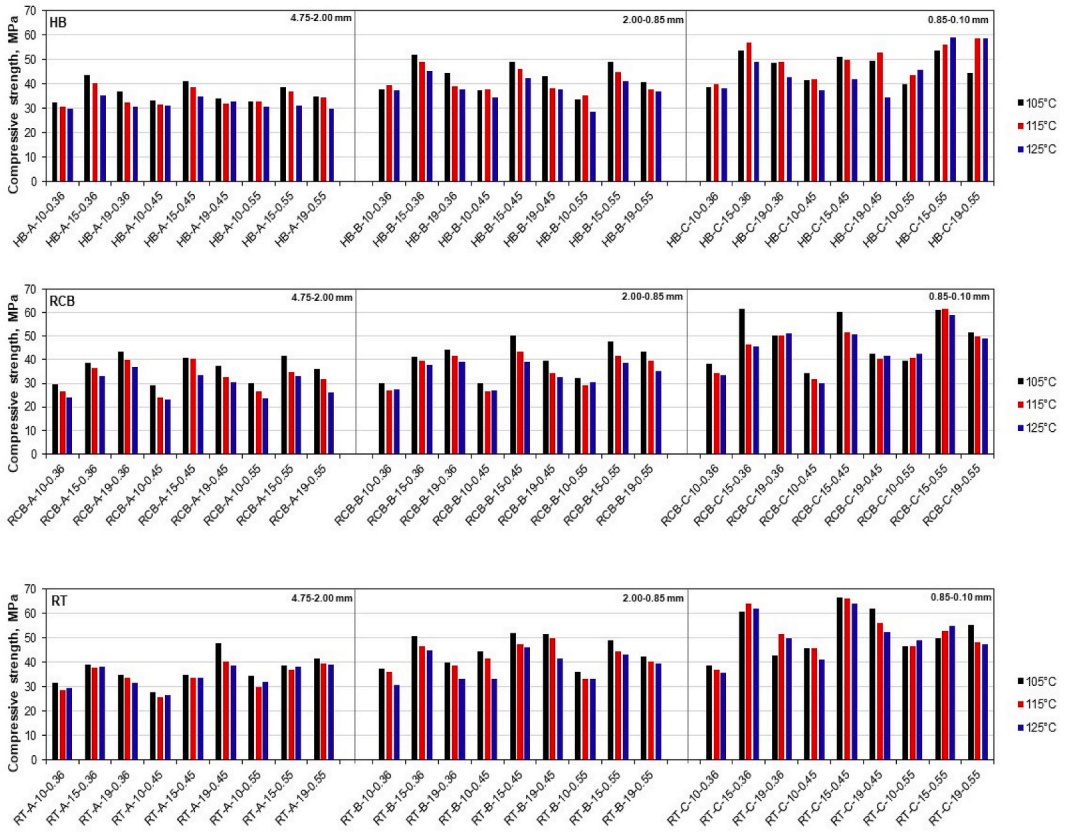

Fig. 6. Compressive strength results of CDW-based geopolymer mortars.

Table 6
Pearson Correlation for the compressive strength results of the geopolymer mortars strength with RCA size, curing temperature, NaOH molarity, and RCA/binder ratio.

Precursor		RCA size	NaOH molarity	Temperature	RCA/binder
HB	Pearson Correlation	−0.679	0.261	−0.198	−0.001
	Sig. (2-tailed)	0.000	0.019	0.076	0.991
	N	81	81	81	81
RCB	Pearson Correlation	−0.555	0.462	−0.243	0.048
	Sig. (2-tailed)	0.000	0.000	0.029	0.669
	N	81	81	81	81
RT	Pearson Correlation	−0.676	0.357	−0.144	0.052
	Sig. (2-tailed)	0.000	0.001	0.198	0.644
	N	81	81	81	81

chemical compositions, which are crucial for promoting geopolymerization [37]. However, the total amount of siliceous and aluminous oxides of all precursors are almost identical (Table 2). In summary, it was confirmed that any CDW-based masonry could be successfully used as a precursor in geopolymer synthesis regardless of the origin as long as finely ground enough.

3.1.2. *Effect of RCA size*

A significant amount of fine powder is generated while crushing RCA, accounting for around 15–20% of total CW [38]. Thus, it is crucial to focus on increasing the RCA replacement level rather than avoiding its use for the sake of sustainability. However, aggregate size plays a critical role in the mechanical properties of geopolymers, similar to cementitious materials. Moreover, fine RCA usage has more impact than natural sand due to parameters related to old adhered mortar, such as ITZ properties and high water absorption [39]. Regardless of all other parameters except aggregate size, the average compressive strengths of CDW-based geopolymer mortars with the use of 4.75–2.00 mm, 2.00–0.85 mm, and 0.85–0.10 mm sized RCA were 33.9 MPa, 39.6 MPa, and 48.3 MPa, respectively. RCA size was the most dominant parameter on the compressive strength, which can also be easily concluded from the Pearson correlation coefficients given in Table 6. These coefficients were −0.679, −0.555, and −0.676 for HB, RCB, and RT precursors, which were indicative of a strong relationship between strength and RCA size. Compressive strength significantly improved as the RCA size decreased. Main reason for the increased strength is the particle packing effect of smaller-sized RCA, resulting in a denser matrix [40].

Another reason is the improvement in ITZ characteristics with the reduced RCA size, which is directly linked with compressive strength [41]. This improvement will be further detailed in the following sections.

3.1.3. Effect of NaOH concentration

In relation to the results shown in Fig. 6, mortars prepared with 15 M NaOH solution reached the highest strength results. Regardless of other parameters, CDW-based geopolymer mortars activated with 10 M, 15 M, and 19 M NaOH solutions yielded 34.2 MPa, 46.0 MPa, and 41.6 MPa average compressive strength, respectively. As a general trend, it was observed that the compressive strength sharply increased from 10 M to 15 M, while there was a slight decrease when further increased to 19 M. For instance, for RT-C-10-0.45, RT-C-15-0.45, and RT-C-19-0.45 specimens cured at 115 °C, the compressive strength results were 45.5 MPa, 66.2 MPa, and 61.9 MPa, respectively. Most mixtures followed a similar trend (Fig. 6). Indeed, the mechanical characteristics of geopolymers strengthen with increasing hydroxide concentration in solution. However, this enhancement is not constant; rather, there is an optimum alkali concentration range, which allows for a higher level of silica and alumina leaching [42]. If the molarity of the hydroxide solution exceeds the optimum alkali concentration range, the mechanical properties decline due to the increased viscosity, which makes the leaching of Si and Al atoms difficult [6]. On the contrary, using low-concentration NaOH solution causes poorer geopolymerization due to inadequate alkalinity, which reduces the dissolution rate of Si and Al. As the concentration of hydroxide solution approaches the optimum range, the rate of dissolution rises, resulting in higher strength due to the increased amount of OH^- ions [31]. Consequently, 15 M NaOH solution yielded higher strengths and was the optimum molarity. However, the impact of an alkali solution differs by precursor. For instance, RCB had the highest Pearson Correlation coefficient of 0.462, while this was 0.261 and 0.357 for HB and RT, respectively (Table 6). This showed that the relation between strength and molarity of NaOH solution was more prominent in RCB compared to other precursors. Since the particle fractions of RCB were coarser than others, the effect of fineness on compressive strength seems to differ depending on the NaOH molarity.

3.1.4. Effect of curing temperature

Curing temperature is one of the most critical factors affecting the mechanical properties of geopolymers due to its role in controlling reaction rate [43]. According to our results, the optimum curing temperature was 105 °C as the highest average compressive strength results was noted at this temperature in most cases. The results dropped to 40.7 MPa and 38.4 MPa for specimens cured at 115 °C and 125 °C, respectively. In general, there was a decremental tendency in the compressive strength with the increased temperature levels. It is however of importance to note that for the precise confirmation of this statement, the levels of predetermined curing temperatures are important. According to literature, at lower curing temperatures, the increase in temperature (up to 110 °C) mostly improves the strength measurements of CDW-based geopolymeric materials [10,11,44]. Thus, there seems to be an optimum temperature range for strong geopolymerization rather than a linear relationship, similar to alkali activator molarity. When the curing temperature exceeds this threshold, compressive strength gradually decreases due to the deterioration of reaction products [44], formation of cracks and drying shrinkage [45], or loss of humidity required for polymerization [46]. Conversely, the dissolution of silica and alumina decelerates at low curing temperatures or ambient conditions, resulting in slower poly-condensation with weak paste properties [6].

3.1.5. Effect of RCA/binder ratio

Average compressive strengths of mortars with RCA/binder ratios of 0.36, 0.45, and 0.55 were 40.2 MPa, 40.6 MPa, and 42.2 MPa, respectively. Although the mortars containing the highest amount of RCA (RCA/binder of 0.55) exhibited slightly better compressive strength, it can be regarded negligible since the differences between the results were very low. As also shown in Table 6, the RCA/binder ratio, which had the smallest Pearson Correlation coefficient among all parameters, was the least effective parameter on compressive strength. Although the RCA replacement ratio significantly affects the mechanical properties of geopolymeric materials [47], it was not that influential in CDW-based geopolymer mortars, considering the replacement ratios used. RCA is mostly substituted with natural aggregates at certain ratios rather than a full replacement. On the contrary, since RCA had already been fully replaced in all mixtures herein, there were no significant changes in compressive strength depending on the RCA/binder ratio. Another point is

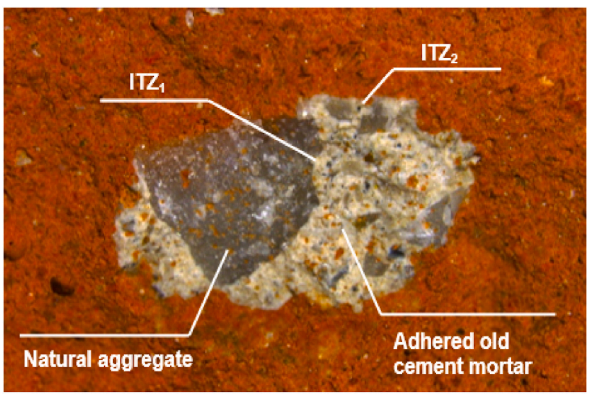

Fig. 7. Sectional view of RCA obtained from RCB-B-15-0.55 mixture.

that the effect of RCA replacement is directly linked to the targeted strength of the material [48]. For instance, in high-strength concrete, mechanical performance is sharply reduced with increased RCA replacement mostly due to failure in weaker adhered old mortar. This may not be observed in concretes with low strength since their ultimate strength depends predominantly on paste properties [48]. According to the results, the CDW-based geopolymer mortars produced in the study can be accepted as moderate-strength mortars (average strength was around 40 MPa). Therefore, this seems to leave the precursor type, molar concentration, curing temperature, and RCA size more important than RCA replacement ratio in regard to strength measurements.

3.2. Interfacial transition zone (ITZ)

In this section, ITZ regions were deeply inspected through line mapping analysis considering the fact that the ITZ properties have a significant impact on compressive strength [49,50]. Fig. 7 presents the sectional view of RCA obtained from the RCB-B-15-0.55 specimen cured at 115 °C. This specimen was selected as it exbited an average compressive strength performance (41.7 MPa), which could provide general information about ITZ. In contrast to natural aggregates, ITZ of RCA with the geopolymer matrix is more complicated [51]. There are two ITZs in the geopolymer matrix when RCA is substituted: the former is the old ITZ between adhered old mortar and original natural aggregates (ITZ_1) and the latter is the new ITZ between new mortar and old mortar connected to the surface of RCA (ITZ_2). This additional ITZ increases the likelihood of fracture and reduces the bond strength [52]. Thus, deep prospecting is needed to investigate the microstructure of matrix in the case of RCA inclusion.

In Figs. 8 and 9, the line mapping analyses with SEM images of the RCA-paste connection of RCB-B-15-0.55 mixture are displayed. The former focuses on the RCA with a 1 mm diameter while the latter focuses on the RCA with a 2 mm diameter. This is for investigating the effect of RCA size, which was the main parameter affecting the compressive strength, on ITZ properties. The ITZ in Fig. 8 was narrower and shallower, which confirms the improvement in compressive strength with smaller aggregates, compared to ITZ shown in Fig. 9. Narrowing of ITZ with the use of smaller RCA was also stated in previous studies [53,54]. Another striking point is the difference in the sharpness of changes in ITZ regions between the RCA and paste. In line with mapping analyses in Fig. 8-c, the changes in Ca and Si intensities at ITZ regions are gradual, which indicates for a soft transition and similarity between different phases while the same intensities change sharply in Fig. 9-c, implying for clearer differences in the RCA and paste phases and weaker bonding, which decreases compressive strength. The thinner ITZ in smaller RCA however explains the higher compressive strength.

4. Life cycle assessment of CDW-based geopolymer mortars

4.1. Description of the system for LCA

The LCA analysis framework was divided into 3 main stages according to the ISO 14040 and ISO 14044 standards [55,56]. The goal

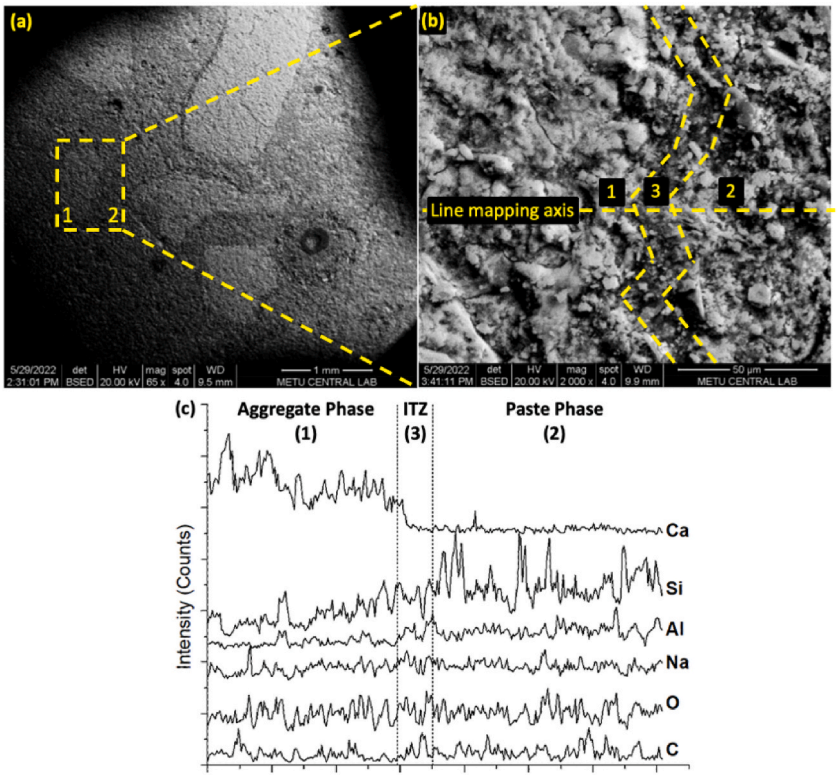

Fig. 8. SEM images of RCA/paste connection (a) an area [65 ×] containing both RCA (1 mm) (1) and geopolymer paste (2), (b) zoomed view [2000 ×] of yellow dotted area plotted in (a) (lines point out the ITZ), (c) mapping analysis of line through RCA, ITZ, and paste.

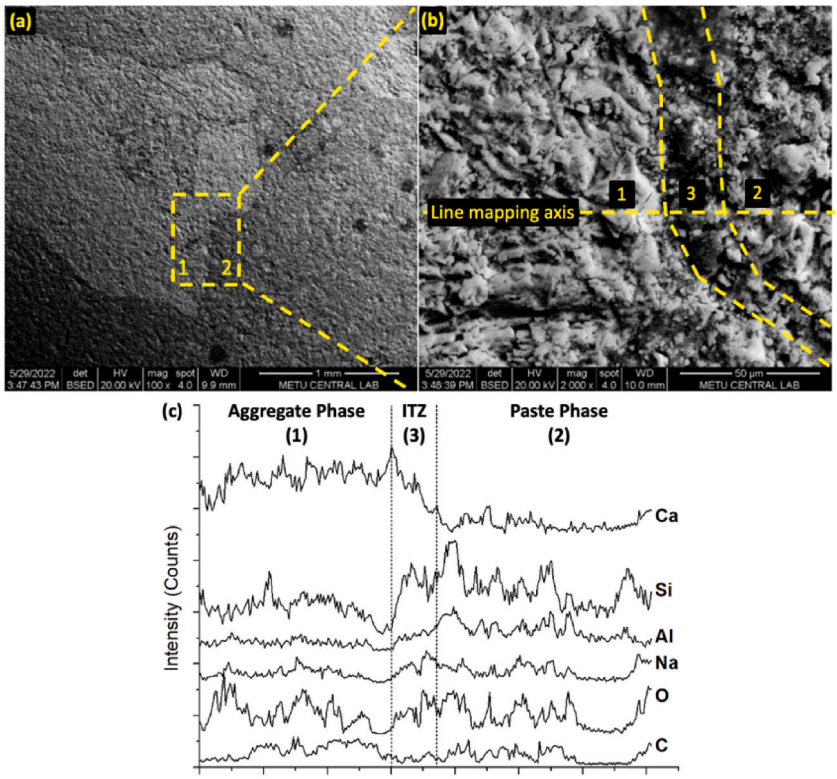

Fig. 9. SEM images of RCA/paste connection (a) an area [100 ×] containing both RCA (2 mm) (1) and geopolymer paste (2), (b) zoomed view [2000 ×] of yellow dotted area plotted in (a) (lines point out the ITZ), (c) mapping analysis of line through RCA, ITZ, and paste.

and scope of the study, system boundaries, and functional unit were determined in the first stage. In the second stage, which included the creation of the inventory analysis, the material-energy consumptions and waste-emission productions were defined. In the last stage, the environmental impacts of geopolymer mortars were identified according to various impact categories. The stages of LCA are detailed in the following sections.

4.2. Goal and scope of the LCA study

The current LCA study was performed to highlight the environmental impact of the CDW-based geopolymer mortars and reveal their pros and cons against the PC-based conventional systems. For this purpose, a base mixture from CDW-based geopolymer mortar mixtures, which were produced to investigate compressive strength, was selected, and an Portland cement-fly ash-based mortar (PCF) mixture with the similar compressive strength class (an aerage of 47.4 MPa at 28 days) was produced to enable comparison. The reasons behind selecting such a mortar for the comparison are the fly ash content, which allows the comparison of a by-product's environmental impact, and the similarity in both mechanical performances and aggregate content. Since the developed geopolymer mortars are intended for use in developing geopolymer composites in further studies, the design parameters were determined to be similar to a conventional PCF mortar. Fig. 10 shows the mixtures used for LCA analysis. The selection methodology of the mixtures was carried out according to following steps.

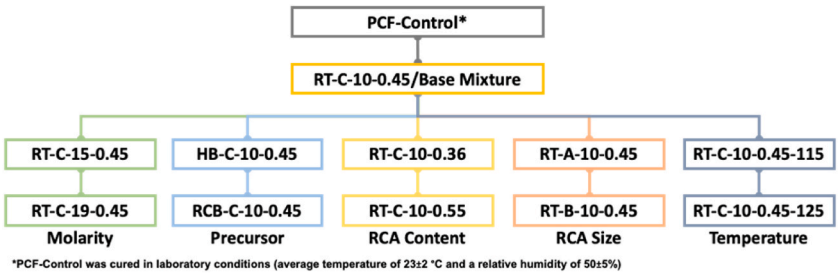

Fig. 10. Selected PCF and CDW-based geopolymer mortars for LCA.

(i) RT-C-10-0.45 was chosen as the base mixture with an average compressive strength of 44.0 MPa for different curing temperatures in RT-C, the group with the highest average compressive strength independent of all parameters.
(ii) In order to examine the environmental impacts of molarity, versions of the base mixture with different molarities (RT-C-15-0.45 and RT-C-19-0.45) were selected.
(iii) Impacts of the binder phase were investigated by the versions of the base mixture prepared with different binder types with the same mixing ratios (HB-C-10-0.45 and RCB-C-10-0.45).
(iv) Versions of the base mixture with different RCA/binder contents (RT-C-10-0.36 and RT-B-10-0.45) were included in the analysis to evaluate the impact of RCA content, while versions containing the different sizes of RCA were chosen to compare the particle size impact of RCA (RT-A-10-0.45 and RT-B-10-0.45).
(v) To reveal the environmental impacts of thermal curing, the versions of the base mixture subjected to different curing temperatures (105 °C, 115 °C, and 125 °C) were selected.

A system boundary was determined for the production of CDW-based geopolymer mortar, covering transportation, processing, mixing, and curing. The functional unit of the analysis, that was performed with the cradle-to-gate approach was determined to be "1 m^3 of CDW-based geopolymer mortar". Fig. 11 depicts the system boundary of the CDW-based geopolymer mortar production. In line with the cradle-to-gate approach; the initiation of the system was the transportation of the CDW elements to the laboratory. Thereafter, the processing of masonry precursors and waste concrete-based RCA, including the crushing, grinding/sieving stages (grinding for masonry and sieving for waste concrete), were followed. The alkali activator's components, NaOH and water were added to the mixing stage of the system. After the mixing stage, the thermal curing process was included. Finally, the system boundary was completed by performing the energy consumption-waste/emissions assignments. For the production of PCF mortar, all ingredients were purchased from suppliers at different locations, and a system boundary was not defined in detail due to a lack of the production details of ingredients. Therefore, only the transportation and production (mixing stage) data of PCF mortar was integrated into the calculations.

4.3. Life cycle inventory (LCI)

LCI of CDW-based geopolymer mortar mixtures was adopted from the experimental studies on a lab-scale, and to make a realistic comparison to the PCF mortar; related data was scaled up to an industrial scale through adopting the industrial scale versions of lab-scale equipments for processing of geopolymers. The main reason behind this approach is that the existing database of cement and silica sand, which are the components of PCF, is based on industrial-scale production procedures, and data on the processing of CDW elements is not available. The transportation and material flows of CDW-based geopolymer mortars are detailed in Table 7 and Table 8, respectively. Transportation distances were determined via using Google Maps. Depending on the quantity of each material, different types of freight are calculated in tkm (Table 7). CDW-based precursors were transported from different demolition sites in Ankara, Turkey, while the Portland cement and silica sand were purchased from a supplier 15.2 km from the laboratory, and the alkali activator was purchased from a supplier 13.4 km away.

Table 8 presents the material quantities required for the production of 1 m^3 CDW-based and PCF mortar. To produce the PCF mortar, ordinary PC with a strength class of 42.5 and silica sand was used. Since the SimaPro databases do not contain country-specific data for Turkey on material and energy consumption or emissions caused by these materials throughout their life cycles, the existing data on cement and silica sand were taken into consideration. In this respect, the averaged transformation and market data for different regions were factored into the equation, considering the fact that the data available for cement and silica sand in the databases varied

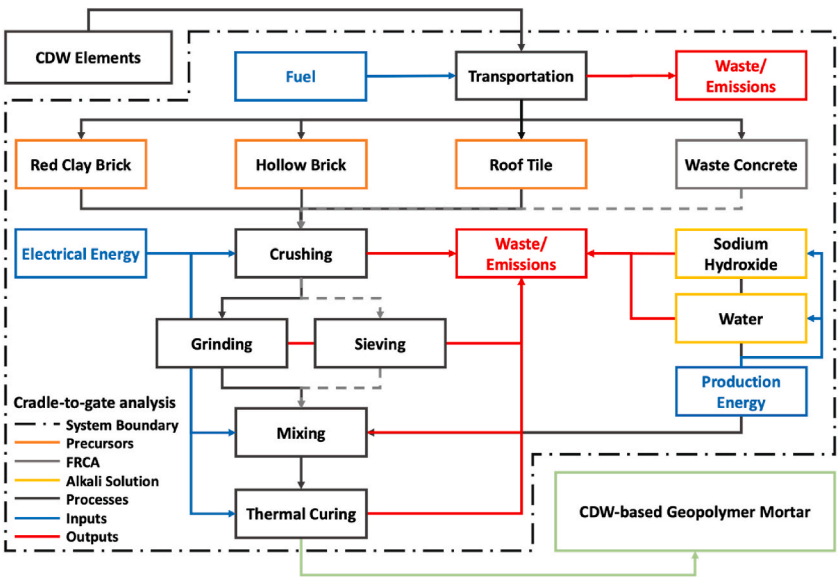

Fig. 11. System boundary to manufacture 1 m^3 of CDW-based geopolymer mortars.

Table 7
Transportation inventory for CDW-based geopolymer mortars.

Material	Distance (km)	Freight (tkm)[a]
Portland cement	15.20	1.12
Fly ash	553.8	49.1
Silica sand	15.20	0.89
Superplasticizer	14.20	0.01
Roof tile	10.90	1.47
Red clay brick	9.400	1.27
Hollow brick	10.90	1.48
Concrete waste	12.10	0.73
Sodium hydroxide	13.40	0.28

[a] Calculated according to the criteria of "amount of material in ton transported over a specified distance".

Table 8
Inventory input material flows for PCF and CDW-based geopolymer mortars.

PCF mortar ingredients (kg/m^3)							
Mixture ID	PC[a]	FA[a]	SS[a]	SP[a]	W[a]		Total
PCF-Control	554.3	665.2	439.0	4.3	329.3		1992.2
Specific gravity	3.06	2.10	2.60	1.10	1.00		
Geopolymer mortar ingredients (kg/m^3)							
Comparision Parameters	Mixture ID	RT[a]	RCB[a]	HB[a]	CW[a]	SH[a]	W[a]	Total
Molarity	RT-C-10-0.45	1014.5	–	–	456.5	141.1	355.1	1967.2
	RT-C-15-0.45	981.9	–	–	441.9	205	343.7	1972.4
	RT-C-19-0.45	958.9	–	–	431.5	250.2	335.6	1976.1
Precursor	RT-C-10-0.45	1014.5	–	–	456.5	141.1	355.1	1967.2
	HB-C-10-0.45	–	–	1019.7	458.9	141.8	356.9	1977.3
	RCB-C-10-0.45	–	1013.2	–	455.9	140.9	354.6	1964.6
RCA content	RT-C-10-0.36	1060.4	–	–	381.7	147.5	371.1	1960.7
	RT-C-10-0.45	1014.5	–	–	456.5	141.1	355.1	1967.2
	RT-C-10-0.55	968	–	–	532.4	134.6	338.8	1973.7
RCA size	RT-A-10-0.45	1045.1	–	–	470.3	145.4	365.8	2026.5
	RT-B-10-0.45	1034.8	–	–	465.6	143.9	362.2	2006.5
	RT-C-10-0.45	1014.5	–	–	456.5	141.1	355.1	1967.2
Thermal curing	RT-C-10-0.45	1014.5	–	–	456.5	141.1	355.1	1967.2
	RT-C-10-0.45[b]	1014.5	–	–	456.5	141.1	355.1	1967.2
	RT-C-10-0.45[c]	1014.5	–	–	456.5	141.1	355.1	1967.2
Specific gravity		2.80	2.79	2.84	2.29[d]	2.13	1.00	

[a] PC: Portland cement, FA: Fly ash, SS: Silica sand, SP: Superplasticizer, RT: Roof tile, RCB: Red clay brick, HB: Hollow brick, CW: Concrete waste, SH: NaOH, W: Water.
[b] Related mixture was subjected to thermal curing at 115 °C.
[c] Related mixture was subjected to thermal curing at 125 °C.
[d] Average value for RCAs (RCA-A: 2.44; RCA-B: 2.32; RCA-C: 2.10).

according to the regions. In addition, the wide availability and accessibility of construction and demolition wastes globally are other main reasons for the holistic approach to PCF mortar, which is executed by using the average data obtained from different regions in the databases. The data used for the analysis were determined according to transformation datas of *Switzerland, Europe without Switzerland, the United States, Canada-Quebec, and the Rest of the World* for cement, and based on *Global, and Rest of the World* for silica sand. There is no data in the databases on behalf of the production process for the waste masonry that form the precursor phase of CDW-based geopolymer mortars. Because of this, the energy input for the precursor phase was only determined using the energy consumption data of the equipment employed in the pre-processing (crushing & grinding) that was carried out to prepare the materials for alkali activation. Similar to that, the inputs for the RCA were determined by taking the pre-processing into account (crushing & sieving). Since there is no country-specific data for the NaOH used as the alkali activator, *Sodium Hyroxide-Rest of the World* data in SimaPro was included in the calculations. *Tap water, Rest of the World (production with underground water without treatment)* data was used for water, the other component of the alkali activator.

Table 9 presents input energy flow data for mixtures. Only the mixing operation that was performed to prepare the mixtures was considered as the energy consumption input, while no additional input was allocated for the curing phase due to the ambient curing for PCF mortar. In addition to the energy inputs for the pre-treatments and mixing procedure for preparing the precursor and RCA, the energy input for the applied heat curing was included in the analysis for CDW-based geopolymer mortars. Total electrical energy consumed during the working period was computed based on the hourly electricity consumption information to determine the energy input for the equipment. Relevant calculations have been scaled-up by using capacity and consumption data of industrial-scale versions of the equipment used in the lab-scale production. For example, the pre-crushing to make CDW ready for grinding was performed by a lab-scale jaw crusher with a power consumption of 1.5 kW; 3.5 kg of raw CDW was crushed in 5 min and loaded into a ball mill

Table 9
Inventory input energy flows for PCF and CDW-based geopolymer mortars.

Comparision parameters	Mixture ID[a]	Energy Consumption (MJ)									
		Precursor Preparation		RCA Preparation				Production & Curing (°C)			
		C	G	RCA-A	RCA-B	RCA-C	S	M	105	115	125
	PCF-Control	–	–	–	–	–	–	5.7	–	–	–
Molarity	**RT-C-10-0.45**	2.7	51.1	–	–	1.5	2.5	5.5	17.2	–	–
	RT-C-15-0.45	2.7	49.5	–	–	1.4	2.4	5.6	17.3	–	–
	RT-C-19-0.45	2.6	48.3	–	–	1.4	2.3	5.6	17.3	–	–
Precursor	**RT-C-10-0.45**	2.7	51.1	–	–	1.5	2.5	5.5	17.2	–	–
	HB-C-10-0.45	2.8	51.4	–	–	1.5	2.5	5.6	17.3	–	–
	RCB-C-10-0.45	2.7	51.1	–	–	1.5	2.5	5.5	17.2	–	–
RCA content	**RT-C-10-0.36**	2.9	53.4	–	–	1.2	2.1	5.5	17.2	–	–
	RT-C-10-0.45	2.7	51.1	–	–	1.5	2.5	5.5	17.2	–	–
	RT-C-10-0.55	2.6	48.8	–	–	1.7	2.9	5.6	17.3	–	–
RCA size	**RT-A-10-0.45**	2.8	52.7	1.3	–	–	2.5	5.7	17.7	–	–
	RT-B-10-0.45	2.8	52.2	–	1.4	–	2.5	5.6	17.6	–	–
	RT-C-10-0.45	2.7	51.1	–	–	1.5	2.5	5.5	17.2	–	–
Thermal curing	**RT-C-10-0.45**	2.7	51.1	–	–	1.5	2.5	5.5	17.2	–	–
	RT-C-10-0.45[b]	2.7	51.1	–	–	1.5	2.5	5.5	–	17.7	–
	RT-C-10-0.45[c]	2.7	51.1	–	–	1.5	2.5	5.5	–	–	18.3

[a] C: Crushing, G: Grinding, RCA: Recycled concrete aggregate, RCA-A, B, C: RCA particle size (A:4.75–2.00 mm, B: 2.00–0.85 mm, C: 0.85–0.10 mm), S: Sieving, M: Mixing.
[b] Related mixture was subjected to thermal curing at 115 °C.
[c] Related mixture was subjected to thermal curing at 125 °C.

with a power consumption of 1.5 kW for an hour to perform the grinding. Since this process requires a large number of iterations for the production of 1 m^3 CDW-based geopolymer mortar and does not realistically reflect the energy consumption caused by the material's life cycle, the energy consumption calculations were based on the production capacity and power consumption of the industrial-scale versions of the equipments. In this context, the power consumption values for the selected industrial-scale ball mill, crusher, siever, and mixer were 280 kW, 15 kW, 7.4 kW, and 190 kW, respectively. Working capacity for the ball mill and crusher, siever, and mixer were 20 tons, 10 tons, and 120 m^3, respectively. For the thermal curing, a 180 kW industrial walk-in oven with a volume of 21.7 m^3 was chosen. Electricity data for the types of equipment were modeled on the basis of the Turkey grid mix in the SimaPro database [57].

4.4. Environmental impact assessment

Depending on the LCI analysis, the environmental impacts of CDW-based geopolymer and PCF mortars were determined with SimaPro 9.0 and the Ecoinvent 3.0 embedded database. For the environmental assessment, the TRACI 2.1 V1.05/US 2008 (Tool for Reduction and Assessment of Chemicals and Other Environmental Impacts) method was used [58]. Environmental impacts selected to be analyzed were Global Warming Potential (GWP), Ozone Depletion Potential (ODP), Acidification Potential (AP), Eutrophication Potential (EP), and Fossil Fuel Depletion (FFD). The GWP, which reflects the ability to retain heat relative to CO_2 over a hundred-year period, is a reference indicator of the greenhouse impact causing global warming [59]. The ODP is the amount of ozone destroyed by a vapor emission over its entire atmospheric lifetime in comparison to the same mass of CFC-11 emission [60]. As a consequence of the increased ultraviolet (UV) radiation due to stratospheric ozone layer depletion [58], ecosystems and human life may be impacted [61]. Acidification, which can affect humans, animals, ecosystems, soil, and ground-surface waters, is caused by sulfur dioxide (SO_2), nitrous oxides (NO_x), and reduced nitrogen (NH_x) generated by fossil fuel combustion [58]. The AP indicates the total amount of acidic pollutants, including SO_2, NO_x, and NH_x, that have contaminated soil, groundwater, surface water, ecosystems, and other materials [62]. Eutrophication is a phenomenon that causes an overabundance of algae and plants due to the enrichment of nutrients, especially nitrogen and phosphorus, from polluted emissions, wastewater, and fertilizers [63]. EP represents the total nitrogen emissions from overfertilization that have an adverse effect on the terrestrial and aquatic ecosystems [64]. While this phenomenon reduces the oxygen and solar energy rates in aquatic eutrophication, it causes pollution of plants and groundwater in terrestrial eutrophication [63]. FFD is the TRACI methodology's energy usage indicator with the megajoule (MJ) surplus unit, which reflects how much more energy will be required in the future to extract one unit of fossil fuel [65].

4.4.1. Life cycle impact assessment (LCIA)

The environmental impact assessment results of PCF and CDW-based geopolymer mortars are presented in Table 10 and illustrated in Fig. 12. At first sight, the promising impact results of CDW-based geopolymer mortars in all categories can be recognized, except for the ODP and EP. GWP, the most critical and highly weighted impact category according to the European Commission [66], was found significantly lower for all geopolymer mortars compared to the PCF control mixture. The AP values were also significantly lower than the PCF mortar for all geopolymer mortars; while the FFD values were found to be similar to PCF mortar except for mixtures produced with high alkali activator content (RT-C-15-0.45 and RT-C-19-0.45). Reflecting the benefits of recycling waste on environmental impacts to a large extent, geopolymer mortars had 65.9% less GWP, 34.3% less AP compared to the PCF. Besides, the

Table 10
Environmental impact assessment results of PCF and CDW-based geopolymer mortars.

Comparision Parameters	Impact category	Ozone depletion potential (ODP)	Global warming potential (GWP)	Acidification potential (AP)	Eutrophication potential (EP)	Fossil fuel depletion (FFD)
	Unit	kg CFC-11 eq	kg CO_2 eq	kg SO_2 eq	kg N eq	MJ surplus
	PCF-Control	2.04E-05	501.1	1.37	0.564	194.2
Molarity	**RT-C-10-0.45**	11.5E-05	178.7	0.941	1.188	186.1
	RT-C-15-0.45	16.7E-05	251.4	1.330	1.679	260.1
	RT-C-19-0.45	20.3E-05	302.8	1.605	2.025	312.5
Precursor	**RT-C-10-0.45**	11.5E-05	178.7	0.941	1.188	186.1
	HB-C-10-0.45	11.6E-05	179.6	0.946	1.194	187.1
	RCB-C-10-0.45	11.5E-05	178.3	0.940	1.187	185.5
RCA content	**RT-C-10-0.36**	12.0E-05	186.3	0.982	1.240	193.9
	RT-C-10-0.45	11.5E-05	178.7	0.941	1.188	186.1
	RT-C-10-0.55	11.0E-05	171.0	0.900	1.136	178.2
RCA size	**RT-A-10-0.45**	11.9E-05	184.0	0.969	1.224	191.6
	RT-B-10-0.45	11.8E-05	182.2	0.960	1.212	189.7
	RT-C-10-0.45	11.5E-05	178.7	0.941	1.188	186.1
Thermal curing	**RT-C-10-0.45**	11.5E-05	178.7	0.941	1.188	186.1
	RT-C-10-0.45[a]	11.5E-05	178.8	0.942	1.189	186.2
	RT-C-10-0.45***	11.5E-05	178.9	0.942	1.190	186.3

*Related mixture was subjected to thermal curing at 115 °C.
[a] Related mixture was subjected to thermal curing at 125 °C.

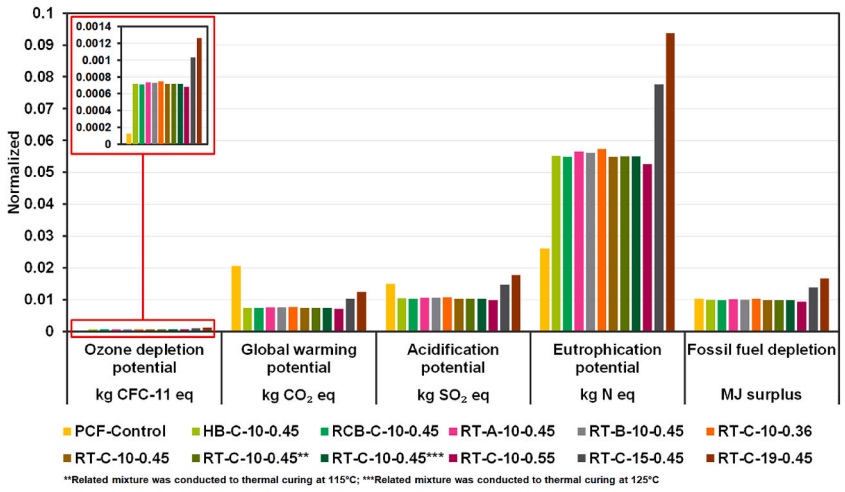

Fig. 12. Normalized environmental impact assessment results of PCF and CDW-based geopolymer mortars.

geopolymerization technique ensured a 8.2% lower FFD than the PCF, demonstrating that the FFD could be reduced with further optimization. For ODP and EP values, the PCF mortar exhibited the lowest environmental impact compared to the geopolymer mortars. ODP related outputs mainly resulted from the chlor-alkali process in the NaOH production, which covers the usage of carbon

tetrachloride to recover chlorine from gas streams [67,68].

4.4.2. Contribution analysis

At this stage, along with the assessment of the environmental impacts of the selected mixtures discussed above, contribution analysis was performed to evaluate the contribution of each component to the environmental impact categories individually. As can be inferred from Fig. 13, the PC was found responsible for approximately 63.7% of the FFD for the PCF-control mixture, whereas this ratio increased up to 93.2% for other environmental impacts. This contribution was followed by the FA, with a contribution rate varied between 4.5 and 28.1%, while highest contributions were noted for the ODP and FFD. Considering that only transportation data was included for the FA, this result was expected since the transportation process directly requires the diesel used in lorries which is responsible for the execrations of fossil and higher CO_2 emissions and eventually makes ODP and FFD more sensitive compared to other environmental impact categories [69].

On the other hand, in the RT-C-10-0.45 coded geopolymer base-mixture, it was observed that NaOH was responsible for at least 88.18% of the calculated environmental impact values considering all categories. Contribution of NaOH to ODP is calculated as 98.78% and this situation is associated with the release of tetra-chloro methane into the atmosphere, which may damage the ozone layer, due to the electrolysis process during the production of NaOH [68]. While the highest impact in the AP, EP, GWP, and FFD categories after NaOH was found to be driven by the grinding process with values ranging from 4.8 to 5.2%, its impact on the ODP was not noteworthy. Apart from these parameters, thermal curing, which causes environmental effects to be responsible only for electricity consumption, showed a similar proportional distribution but lesser impact than grinding.

In the following section, the environmental impacts of the differentiation in the parameters such as precursor types, alkali activator content, RCA content/size, and thermal curing are presented in Figs. 14–18, respectively. In each figure, examined material or process was highlighted with dashed lines. According to Fig. 14, considering that RT, HB, and RCB were subjected to the same crushing-grinding processes and all other remaining parameters (*i.e.*, alkali activator, thermal curing, RCA, etc.) were applied at the same rate and type, it can be stated that different values obtained in the environmental impact categories may be attributed only to the specific gravity of different types of precursors (Table 8) and, accordingly, the different weights of the mixtures to be produced in the same volume. For instance, according to Tables 8 and it was seen that a total of 1977.3 kg of material was used in the RCB-based mixture, 1967.2 kg in the RT-based mixture, and 1964.6 kg in the HB-based mixture to produce 1 m^3 of geopolymer, and these values were in the same trend with the values calculated for all environmental impact categories.

Fig. 15 depicts the contribution of materials and processes to environmental impacts from a molarity point of view. According to Fig. 15a, it can be stated that the molarity concentration had a dominant influence on the environmental impacts of geopolymers for all impact categories. The impact factors for 15 M increased by 39.8–44.7% compared to 10 M concentration, and the increment rates for the transition from 15 M to 19 M ranged from 20.1 to 21.9%. The ODP was the category most affected by alkali activator molarity, with at least 98.8% contribution to environmental impacts, while FFD was the least affected category, with at least 88.2% contribution.

According to Fig. 16, an increase in the usage rate of the RCA in geopolymer mortars led to a decrease in environmental burden for all impact categories. However, since the contribution of the RCA usage was significantly lower, the positive impact of the RCA content remained restricted (Fig. 16b). For instance, as the RCA content increased up to 0.45 from 0.36, a reduction in environmental impact, regardless of the category, was noted in the range of 4.0–4.3%. Similarly, an increase in the RCA content from 0.45 to 0.55 resulted in a decrease in environmental impact between 4.2 and 4.6%. In general, it can be stated that the usage of RCA can assist in reducing the environmental burden of geopolymer mortars; however, since the RCA had the lowest contribution, possible advantages would be restricted, and the contribution share of other ingredients and processes would tend to be same with other mixture options.

Fig. 17 demonstrates the contribution of RCA size to the environmental impacts of CDW-based geopolymer mortars. It was expected that using the RCA would cause a reduction in the environmental burden of geopolymer mortars; however, compared to the base mixture (RT-C-10-0.45), the expected behavior was not observed with the increase in RCA size. To obtain RCA with different particle sizes, three RCA crushing processes were performed with different jaw crusher openings, which caused increased energy consumption with the reduction of the RCA size desired to be produced (Table 9). On the other hand, due to decrease in RCA density with the

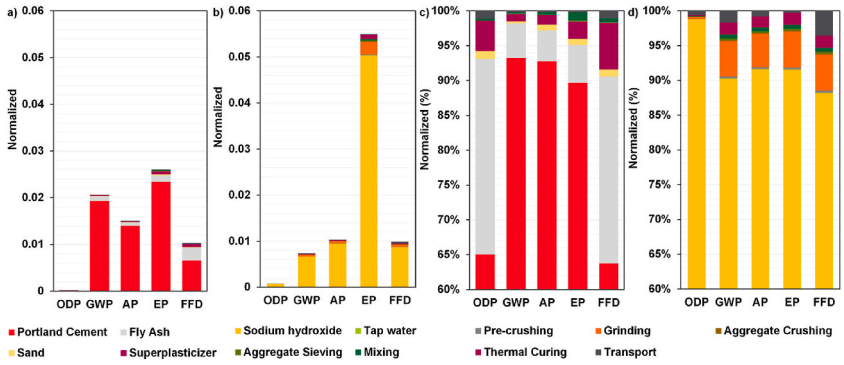

Fig. 13. Environmental impacts of PCF-Control and RT-C-10-0.45 (a) normalized results of PCF-Control (b) normalized results of RT-C-10-0.45 (c) contribution of materials and production processes for PCF-Control (d) contribution of materials and production processes for RT-C-10-0.45.

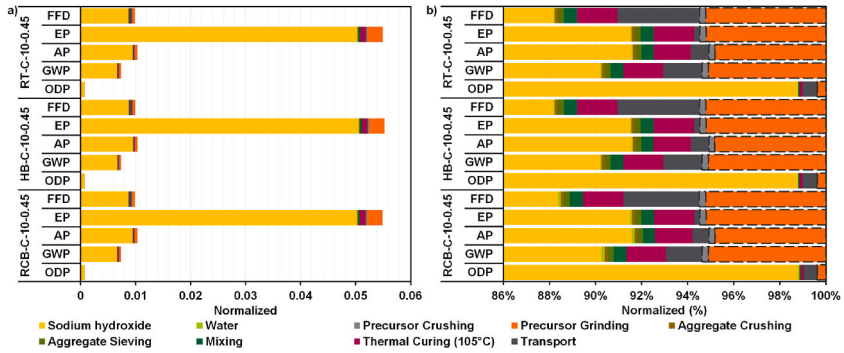

Fig. 14. Environmental impacts of precursor type (a) normalized results (b) contribution of materials and production processes.

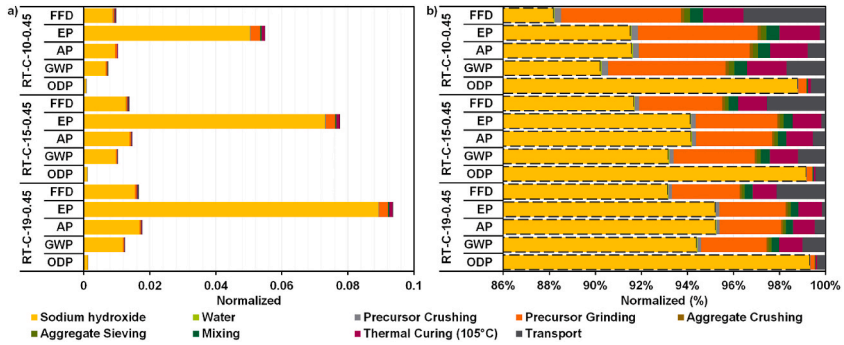

Fig. 15. Environmental impacts of alkali activator content (a) normalized results (b) contribution of materials and production processes.

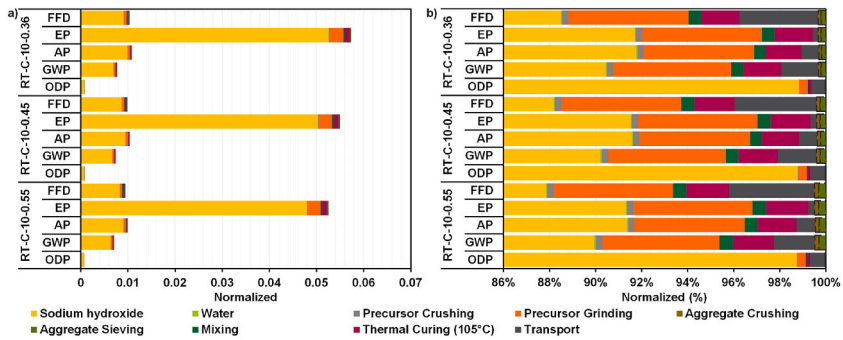

Fig. 16. Environmental impacts of RCA content (a) normalized results (b) contribution of materials and production processes.

reduction in RCA size, the amount of material required to produce 1 m^3 of CDW-based geopolymer mortar was decreased, thus reducing the energy requirement and environmental impacts. Therefore, considering the impacts of RCA content and size on the environment and the mechanical performance, the findings revealed that the optimization of RCA content and size is possible to produce environmentally friendly geopolymer mixtures with high mechanical performance (RT-C-10-0.55 coded mixture with an average compressive strength of 46.3 MPa).

Fig. 18 demonstrates the impact of thermal curing under various temperatures. According to Fig. 18a, it can be stated that the impact of elevated temperatures between 105 and 125 °C slightly changed with negligible increases, as expected considering the energy consumption values (Table 9). Although the change was inconsiderable, thermal curing ranked 3rd or 4th in contributing to environmental impact due to high energy consumption demand in the process (Fig. 18b). On the other hand, significantly lower environmental impacts compared to PCF mortar make the CDW-based geopolymer mortars a promising building material due to their high compressive strength gained in short curing periods. Therefore, it is believed that further optimizations for lower curing temperatures and durations can significantly increase the environmental advantages of CDW-based geopolymer mortars.

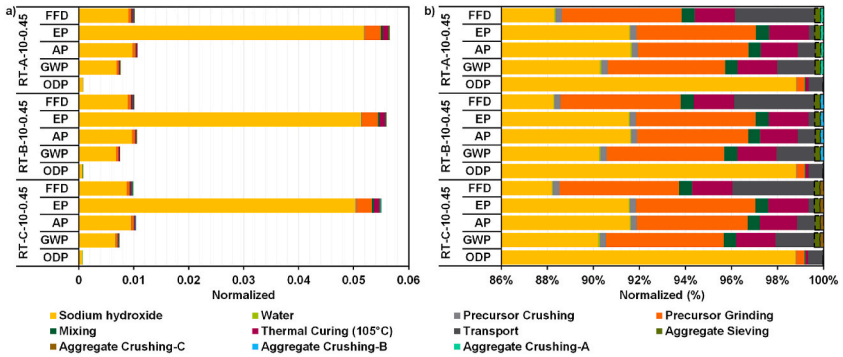

Fig. 17. Environmental impacts of RCA size (a) normalized results (b) contribution of materials and production processes.

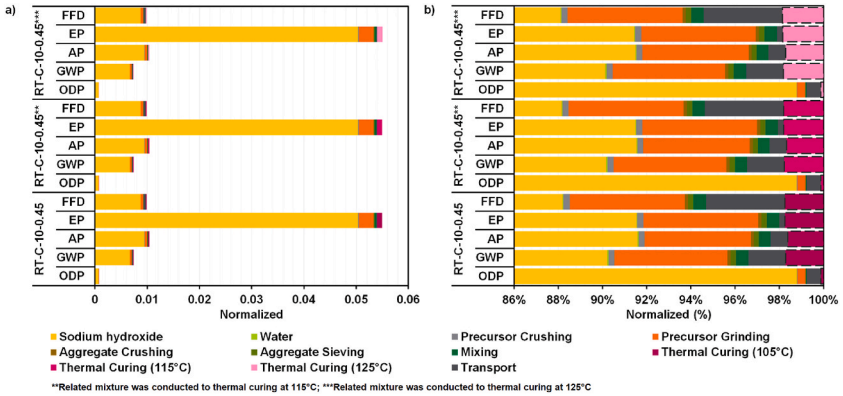

Fig. 18. Environmental impacts of thermal curing (a) normalized results (b) contribution of materials and production processes.

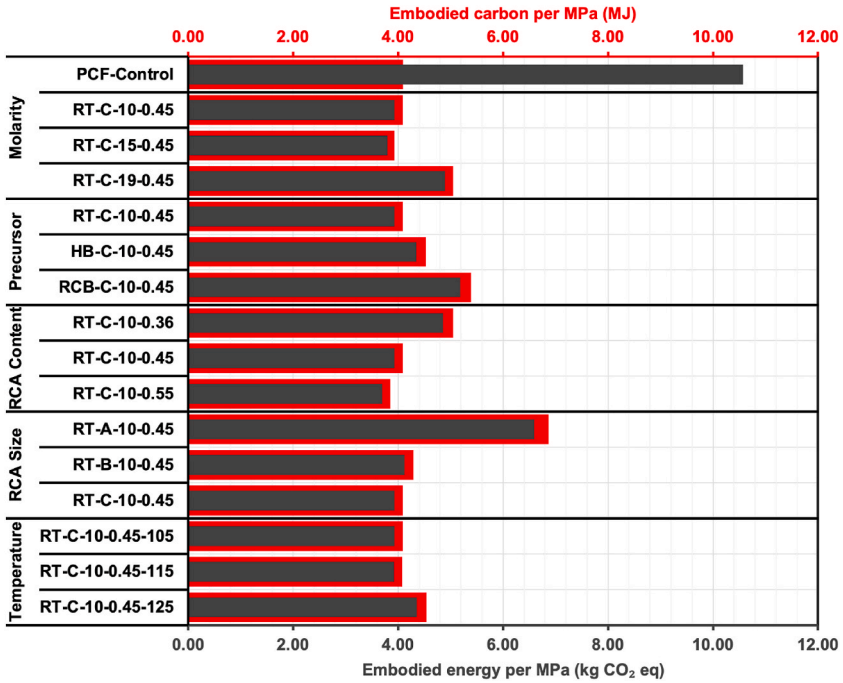

Fig. 19. Embodied energy and carbon per MPa of PCF and CDW-based geopolymer mortars.

4.5. Material sustainability indicators

CDW-based geopolymer and PCF mortars' Material Sustainability Indicators (MSI) are presented in Fig. 19a. MSI is fundamental and easily applicable approach to determine the sustainability degree of materials depending on the amount of carbon and embodied energy of the material per strength development [70]. Similar to LCA analysis, in the determination of MSI values, geopolymer mortars were classified in five different categories according to the strength responsible parameters, including NaOH molarity, precursor type, RCA content and size, and temperature. The findings revealed that PCF-Control contained a drastically high level of embodied carbon per MPa compared to all geopolymer mortars. Compared to the cement-based PCF mortar, the geopolymer base mixture (RT-C-10-0.45), which had the similar strength level as PCF-Control, caused 62.9% less carbon emissions per strength development with a similar energy consumption. According to the paramater related results, the influence of the NaOH molarity change became more prominent for 19 M, while for 10 M and 15 M differed slightly, indicating that the environmental impact of the alkali activator can be taken under control to a certain degree; thus, further optimization of alkali content would be beneficial for geopolymer mortars. The influence of precursor type on the amount of embodied energy and carbon showed an increasing linear trend in the order of RT, HB, and RCB. Considering that the environmental impact of precursor type was highly similar in LCIA, the obtained trend was correlated to the compressive strength development, which was noted as 45.5, 41.3, and 34.4 MPa for RT, HB, and RCB, respectively. The influence of RCA amount on MSI was manifested with an inverse relationship between the increase in the RCA amount and embodied energy/carbon. Up to RCA/binder ratio of 0.55, embodied energy/carbon significantly decreased due to decrease in the alkali activator and precursor amount; in particular, the first was responsible for the highest level of environmental impact. Considering the effect of RCA size, the MSI values declined as the RCA size increased because the dry density of the aggregates reduced, which led to a decrease in the weights of other ingredients required to produce 1 m^3 of geopolymer mortar. The elevated temperatures did not significantly affect the MSI values up to 115 °C, whereas at 125 °C embodied energy/carbon level increased due to an increase in the electricity usage. Considering the average compressive strength results of geopolymer mortars, which were 45.5, 45.6, and 41.1 MPa at 105 °C, 115 °C, and 125 °C, respectively, it was revealed that the production of geopolymers with desired mechanical performance and lower environmental impact could be possible by the proper optimization of curing temperature.

5. Conclusions

This study investigated the single use of HB, RCB, and RT as precursors and the feasibility of full inclusion of RCA (<5 mm) in the production of CDW-based geopolymer mortars subjected to heat curing. Different precursor types, NaOH molar concentrations, RCA sizes, RCA/binder ratios, and curing temperatures were utilized, and the ITZ properties of different-size (1 and 2 mm) RCAs with geopolymer pastes were investigated via SEM imaging coupled with the line mapping analysis in addition to compressive strength tests. According to experimental results, following conclusions can be drawn.

- 100% CDW-based geopolymer mortars were capable of achieving compressive strength of 66.2 MPa after 72-h heat curing. The significant influence of RCA size on compressive strength was confirmed through Pearson correlation, with smaller RCA (0.85–0.10 mm) leading to higher strength levels via improved particle packing.
- On micro-scale, smaller RCAs (1 mm) led to a thinner ITZ in comparison to larger RCAs (2 mm). The alterations in Ca and Si at the ITZ around the larger RCAs resulted in apparent separation and increased vulnerability to fracture. The effect of RCA/binder ratio on the compressive strength of geopolymer mortars was found negligible.
- RT-based geopolymer mortars showed higher compressive strength compared to HB- and RCB-based mortars most probably due to finer particle fractions, as the chemical compositions of the precursors were almost identical.
- NaOH molar concentration was one of the most critical parameters on compressive strength. Mixtures activated with 15 M NaOH generally showed better strength. Excessive concentration led to non-homogeneous microstructure formation, while lower molarity caused limited geopolymerization.
- Among the curing temperatures tested, 105 °C was optimal, temperatures beyond this adversely affected compressive strength due to final product instability and excessive water loss, leading to drying shrinkage and crack susceptibility.
- In the LCA analyses, NaOH had the largest share of environmental impact, followed by the grinding of CDW-based precursors. Transportation and heat curing had the largest impact after NaOH and grinding, depending on the impact category. Optimization of the mixture designs allowed a reduction in GWP and AP by 65.9% and 34.3%, respectively. Geopolymerization method guaranteed an FFD potential 8.2% lower than the PCF. On the contrary, regarding the ODP and EP values, the PCF mortar had the lowest negative burden on the environment.
- For the PC-based mortar with same strength level, the highest environmental impact contribution was noted for the PC. The geopolymer base mixture (RT-C-10-0.45), which had a similar strength to the PC -based control mortar, emitted 62.9% less CO_2 per strength development with similar energy consumption.

Author statement

Anil Kul: Visualization, Investigation, Writing-Original Draft.
Behlul Furkan Ozel: Visualization, Investigation, Writing-Original Draft.
Emircan Ozcelikci: Visualization, Investigation, Writing-Original Draft.
Muhammed Faruk Gunal: Visualization, Investigation, Writing-Original Draft.
Huseyin Ulugol: Writing-Original Draft, Writing-Review & Editing.
Gurkan Yildirim: Conceptualization, Methodology, Resources, Writing-Review & Editing, Supervision, Project administration,

Funding acquisition.

Mustafa Sahmaran: Writing-Review & Editing, Supervision.

Declaration of competing interest

The authors declare that they have no known competing financial interests or personal relationships that could have appeared to influence the work reported in this paper.

Data availability

Data will be made available on request.

Acknowledgements

This project has received funding from the European Union's Horizon 2020 research and innovation programme under the Marie Skłodowska-Curie grant agreement No 894100. The authors also wish to acknowledge the support of the Scientific and Technical Research Council of Turkey (TUBITAK) provided under project: 117M447. This publication is a part of the doctoral dissertation work of the first author at the Hacettepe University, Graduate School of Science and Engineering, Beytepe, Ankara, Turkey.

References

[1] J. Davidovits, False values on CO2 emission for geopolymer cement/concrete published in scientific papers, Technical paper 24 (2015) 1–9.
[2] J.S. van Deventer, J.L. Provis, P. Duxson, D.G. Brice, Chemical research and climate change as drivers in the commercial adoption of alkali activated materials, Waste Biomass Valori 1 (1) (2010) 145–155, https://doi.org/10.1007/s12649-010-9015-9.
[3] P. De Silva, K. Sagoe-Crenstil, V. Sirivivatnanon, Kinetics of geopolymerization: role of Al2O3 and SiO2, Cement Concr. Res. 37 (4) (2007) 512–518, https://doi.org/10.1016/j.cemconres.2007.01.003.
[4] W.P. Zakka, N.H.A.S. Lim, M.C. Khun, A scientometric review of geopolymer concrete, J. Clean. Prod. 280 (2021), 124353, https://doi.org/10.1016/j.jclepro.2020.124353.
[5] P. Zhang, Z. Gao, J. Wang, J. Guo, S. Hu, Y. Ling, Properties of fresh and hardened fly ash/slag based geopolymer concrete: a review, J. Clean. Prod. 270 (2020), 122389, https://doi.org/10.1016/j.jclepro.2020.122389.
[6] M. Alhawat, A. Ashour, G. Yildirim, A. Aldemir, M. Sahmaran, Properties of geopolymers sourced from construction and demolition waste: a review, J. Build. Eng. 50 (2022), 104104, https://doi.org/10.1016/j.jobe.2022.10410.
[7] J.L. Gálvez-Martos, D. Styles, H. Schoenberger, B. Zeschmar-Lahl, Construction and demolition waste best management practice in Europe, Resour. Conserv. Recycl. 136 (2018) 166–178, https://doi.org/10.1016/j.resconrec.2018.04.016.
[8] Y. Shi, J. Xu, BIM-based information system for econo-enviro-friendly end-of-life disposal of construction and demolition waste, Autom. ConStruct. 125 (2021), 103611, https://doi.org/10.1016/j.autcon.2021.103611.
[9] H. Ulugöl, A. Kul, G. Yıldırım, M. Şahmaran, A. Aldemir, D. Figueira, A. Ashour, Mechanical and microstructural characterization of geopolymers from assorted construction and demolition waste-based masonry and glass, J. Clean. Prod. 280 (2021), 124358, https://doi.org/10.1016/j.jclepro.2020.124358.
[10] G. Yıldırım, A. Kul, E. Özçelikci, M. Şahmaran, A. Aldemir, D. Figueira, A. Ashour, Development of alkali-activated binders from recycled mixed masonry-originated waste, J. Build. Eng. 33 (2021), 101690, https://doi.org/10.1016/j.jobe.2020.101690.
[11] E. Ozcelikci, A. Kul, M.F. Gunal, B.F. Ozel, G. Yildirim, A. Ashour, M. Sahmaran, A comprehensive study on the compressive strength, durability-related parameters and microstructure of geopolymer mortars based on mixed construction and demolition waste, J. Clean. Prod. 396 (2023), 136522, https://doi.org/10.1016/j.jclepro.2023.136522.
[12] J. Tan, J. Cai, J. Li, Recycling of unseparated construction and demolition waste (UCDW) through geopolymer technology, Construct. Build. Mater. 341 (2022), 127771, https://doi.org/10.1016/j.conbuildmat.2022.127771.
[13] C. Zhang, M. Hu, M. van der Meide, F. Di Maio, X. Yang, X. Gao, K. Li, H. Zhao, C. Li, Life cycle assessment of material footprint in recycling: a case of concrete recycling, Waste Manag. 155 (2023) 311–319, https://doi.org/10.1016/j.wasman.2022.10.035.
[14] A.T. Gebremariam, F. Di Maio, A. Vahidi, P. Rem, Innovative technologies for recycling End-of-Life concrete waste in the built environment, Resour. Conserv. Recycl. 163 (2020), 104911, https://doi.org/10.1016/j.resconrec.2020.104911.
[15] K. Parthiban, K.S.R. Mohan, Influence of recycled concrete aggregates on the engineering and durability properties of alkali activated slag concrete, Construct. Build. Mater. 133 (2017) 65–72, https://doi.org/10.1016/j.conbuildmat.2016.12.050.
[16] M. Koushkbaghi, P. Alipour, B. Tahmouresi, E. Mohseni, A. Saradar, P.K. Sarker, Influence of different monomer ratios and recycled concrete aggregate on mechanical properties and durability of geopolymer concretes, Construct. Build. Mater. 205 (2019) 519–528, https://doi.org/10.1016/j.conbuildmat.2019.01.174.
[17] S.S. Rahman, M.J. Khattak, Roller compacted geopolymer concrete using recycled concrete aggregate, Construct. Build. Mater. 283 (2021), 122624, https://doi.org/10.1016/j.conbuildmat.2021.122624.
[18] H. Ulugöl, M.F. Günal, İ.Ö. Yaman, G. Yıldırım, M. Şahmaran, Effects of self-healing on the microstructure, transport, and electrical properties of 100% construction-and demolition-waste-based geopolymer composites, Cem. Concr. Compos. 121 (2021), 104081, https://doi.org/10.1016/j.cemconcomp.2021.104081.
[19] H. Ilcan, O. Sahin, A. Kul, G. Yildirim, M. Sahmaran, Rheological properties and compressive strength of construction and demolition waste-based geopolymer mortars for 3D-Printing, Construct. Build. Mater. 328 (2022), 127114, https://doi.org/10.1016/j.conbuildmat.2022.127114.
[20] A. Aldemir, S. Akduman, O. Kocaer, R. Aktepe, M. Sahmaran, G. Yildirim, H. Almahmood A. Ashour, Shear behaviour of reinforced construction and demolition waste-based geopolymer concrete beams, J. Build. Eng. 47 (2022), 103861, https://doi.org/10.1016/j.jobe.2021.103861.
[21] G. Rebitzer, T. Ekvall, R. Frischknecht, D. Hunkeler, G. Norris, T. Rydberg, W.P. Schmidt, S. Suh, B.P. Weidema, D.W. Pennington, Life cycle assessment: Part 1: framework, goal and scope definition, inventory analysis, and applications, Environ. Int. 30 (5) (2004) 701–720, https://doi.org/10.1016/j.envint.2003.11.005.
[22] D.A. Salas, A.D. Ramirez, N. Ulloa, H. Baykara, A.J. Boero, Life cycle assessment of geopolymer concrete, Construct. Build. Mater. 190 (2018) 170–177, https://doi.org/10.1016/j.conbuildmat.2018.09.123.

[23] A. Dal Pozzo, L. Carabba, M.C. Bignozzi, A. Tugnoli, Life cycle assessment of a geopolymer mixture for fireproofing applications, Int. J. LCA. 24 (10) (2019) 1743–1757, https://doi.org/10.1007/s11367-019-01603-z.

[24] G. Kastiukas, S. Ruan, S. Liang, X. Zhou, Development of precast geopolymer concrete via oven and microwave radiation curing with an environmental assessment, J. Clean. Prod. 255 (2020), 120290, https://doi.org/10.1016/j.jclepro.2020.120290.

[25] S. Marinković, J. Dragaš, I. Ignjatović, N. Tošić, Environmental assessment of green concretes for structural use, J. Clean. Prod. 154 (2017) 633–649, https://doi.org/10.1016/j.jclepro.2017.04.015.

[26] L. Nguyen, A.J. Moseson, Y. Farnam, S. Spatari, Effects of composition and transportation logistics on environmental, energy and cost metrics for the production of alternative cementitious binders, J. Clean. Prod. 185 (2018) 628–645, https://doi.org/10.1016/j.jclepro.2018.02.247.

[27] L.K. Turner, F.G. Collins, Carbon dioxide equivalent (CO2-e) emissions: a comparison between geopolymer and OPC cement concrete, Construct. Build. Mater. 43 (2013) 125–130, https://doi.org/10.1016/j.conbuildmat.2013.01.023.

[28] J. Fořt, E. Vejmelková, D. Koňáková, N. Alblová, M. Čáchová, M. Keppert, P. Rovnaníková, R. Černý, Application of waste brick powder in alkali activated aluminosilicates: functional and environmental aspects, J. Clean. Prod. 194 (2018) 714–725, https://doi.org/10.1016/j.jclepro.2018.05.181.

[29] N. Mir, S.A. Khan, A. Kul, O. Sahin, M. Lachemi, M. Sahmaran, M. Koc, Life Cycle Assessment of binary recycled ceramic tile and recycled brick waste-based geopolymers, Cleaner Mater 100116 (2022), https://doi.org/10.1016/j.clema.2022.100116.

[30] N. Mir, S.A. Khan, A. Kul, O. Sahin, E. Ozcelikci, M. Sahmaran, M. Koc, Construction and demolition waste-based self-healing geopolymer composites for the built environment: an environmental profile assessment and optimization, Construct. Build. Mater. 369 (2023), 130520, https://doi.org/10.1016/j.conbuildmat.2023.130520.

[31] K. Komnitsas, D. Zaharaki, A. Vlachou, G. Bartzas, M. Galetakis, Effect of synthesis parameters on the quality of construction and demolition wastes (CDW) geopolymers, Adv. Powder Technol. 26 (2015) 368–376, https://doi.org/10.1016/j.apt.2014.11.012.

[32] D.D. Burduhos Nergis, M.M.A.B. Abdullah, A.V. Sandu, P. Vizureanu, XRD and TG-DTA study of new alkali activated materials based on fly ash with sand and glass powder, Mater 13 (2) (2020) 343, https://doi.org/10.3390/ma13020343.

[33] K.R. Iler, The Chemistry of the Silica: Solubility, Polymerization, Colloid and Surface Properties, and Biochemistry, 1979.

[34] G. Baronio, L. Binda, Study of the pozzolanicity of some bricks and clays, Construct. Build. Mater. 11 (1997) 41–46, https://doi.org/10.1016/S0950-0618(96)00032-3.

[35] ASTM C109, Standard Test Method for Compressive Strength of Hydraulic Cement Mortars (Using 2-in. Or [50-mm] Cube Specimens), ASTM International West, Conshohocken, PA, 2020.

[36] J. Benesty, J. Chen, Y. Huang, I. Cohen, Pearson correlation coefficient, in: Noise Reduction in Speech Processing, İ Springer, Berlin, Heidelberg, 2009, pp. 1–4.

[37] X. Chen, Z. Niu, J. Wang, G.R. Zhu, M. Zhou, Effect of sodium polyacrylate on mechanical properties and microstructure of metakaolin-based geopolymer with different SiO2/Al2O3 ratio, Ceram. Int. 44 (15) (2018) 18173–18180, https://doi.org/10.1016/j.ceramint.2018.07.025.

[38] C. Shi, Z. Wu, Z. Cao, T.C. Ling, J. Zheng, Performance of mortar prepared with recycled concrete aggregate enhanced by CO2 and pozzolan slurry, Cem. Concr. Compos. 86 (2018) 130–138, https://doi.org/10.1016/j.cemconcomp.2017.10.013.

[39] M. Nedeljković, J. Visser, B. Šavija, S. Valcke, E. Schlangen, Use of fine recycled concrete aggregates in concrete: a critical review, J. Build. Eng. 38 (2021), 102196, https://doi.org/10.1016/j.jobe.2021.102196.

[40] A. De Rossi, M.J. Ribeiro, J.A. Labrincha, R.M. Novais, D. Hotza, R.F.P.M. Moreira, Effect of the particle size range of construction and demolition waste on the fresh and hardened-state properties of fly ash-based geopolymer mortars with total replacement of sand, Process Saf. Environ. Protect. 129 (2019) 130–137, https://doi.org/10.1016/j.psep.2019.06.026.

[41] Y. Li, T. Fu, R. Wang, Y. Li, An assessment of microcracks in the interfacial transition zone of recycled concrete aggregates cured by CO2, Construct. Build. Mater. 236 (2020), 117543, https://doi.org/10.1016/j.conbuildmat.2019.117543.

[42] S. Hanjitsuwan, S. Hunpratub, P. Thongbai, S. Maensiri, V. Sata, P. Chindaprasirt, Effects of NaOH concentrations on physical and electrical properties of high calcium fly ash geopolymer paste, Cem. Concr. Compos. 45 (2014) 9–14, https://doi.org/10.1016/j.cemconcomp.2013.09.012.

[43] P. Rovnaník, Effect of curing temperature on the development of hard structure of metakaolin-based geopolymer, Construct. Build. Mater. 24 (7) (2010) 1176–1183, https://doi.org/10.1016/j.conbuildmat.2009.12.023.

[44] M. Tuyan, Ö. Andiç-Çakir, K. Ramyar, Effect of alkali activator concentration and curing condition on strength and microstructure of waste clay brick powder-based geopolymer, Compos. B Eng. 135 (2018) 242–252, https://doi.org/10.1016/j.compositesb.2017.10.013.

[45] L. Biondi, M. Perry, C. Vlachakis, Z. Wu, A. Hamilton, J. McAlorum, Ambient cured fly ash geopolymer coatings for concrete, Mater 12 (6) (2019) 923, https://doi.org/10.3390/ma12060923.

[46] A. Hassan, M. Arif, M. Shariq, Use of geopolymer concrete for a cleaner and sustainable environment–A review of mechanical properties and microstructure, J. Clean. Prod. 223 (2019) 704–728, https://doi.org/10.1016/j.jclepro.2019.03.051.

[47] R.V. Silva, J. De Brito, R.K. Dhir, Prediction of the shrinkage behavior of recycled aggregate concrete: a review, Construct. Build. Mater. 77 (2015) 327–339, https://doi.org/10.1016/j.conbuildmat.2014.12.102.

[48] J. de Brito, R. Kurda, The past and future of sustainable concrete: a critical review and new strategies on cement-based materials, J. Clean. Prod. 281 (2021), 123558, https://doi.org/10.1016/j.jclepro.2020.123558.

[49] C.S. Poon, Z.H. Shui, L. Lam, Effect of microstructure of ITZ on compressive strength of concrete prepared with recycled aggregates, Construct. Build. Mater. 18 (6) (2004) 461–468, https://doi.org/10.1016/j.conbuildmat.2004.03.005.

[50] S. Demie, M.F. Nuruddin, N. Shafiq, Effects of micro-structure characteristics of interfacial transition zone on the compressive strength of self-compacting geopolymer concrete, Construct. Build. Mater. 41 (2013) 91–98, https://doi.org/10.1016/j.conbuildmat.2012.11.067.

[51] D. Xuan, B. Zhan, C.S. Poon, Assessment of mechanical properties of concrete incorporating carbonated recycled concrete aggregates, Cem. Concr. Compos. 65 (2016) 67–74, https://doi.org/10.1016/j.cemconcomp.2015.10.018.

[52] X. Ren, L. Zhang, Experimental study of interfacial transition zones between geopolymer binder and recycled aggregate, Construct. Build. Mater. 167 (2018) 749–756, https://doi.org/10.1016/j.conbuildmat.2018.02.111.

[53] A. Elsharief, M.D. Cohen, J. Olek, Influence of aggregate size, water cement ratio and age on the microstructure of the interfacial transition zone, Cem, Concr. Res. 33 (11) (2003) 1837–1849, https://doi.org/10.1016/S0008-8846(03)00205-9.

[54] K. Lyu, W. She, H. Chang, Y. Gu, Effect of fine aggregate size on the overlapping of interfacial transition zone (ITZ) in mortars, Construct. Build. Mater. 248 (2020), 118559, https://doi.org/10.1016/j.conbuildmat.2020.118559.

[55] ISO Environmental Management-Life Cycle Assessment- Principles and Framework International Organisation for Standardisation, 2006. Geneva, Switzerland.

[56] ISO Environmental Management-Life Cycle Assessment-Requirements and Guidelines International Organisation for Standardisation, 2006. Geneva, Switzerland.

[57] S.A. Khan, A. Kul, O. Şahin, M. Şahmaran, S.G. Al-Ghamdi, M. Koç, Energy-environmental performance assessment and cleaner energy solutions for a novel Construction and Demolition Waste-based geopolymer binder production process, Energy Rep. 8 (2022) 14464–14475, https://doi.org/10.1016/j.egyr.2022.10.345.

[58] U.S. Environmental Protection Agency (EPA, Life Cycle Assessment: Principles and Practice, EPA, Washington, DC, USA, 2006.

[59] LCA measure - global warming potential (GWP) – LCA measure details. https://calculatelca.com/static-content/software/impact-estimator/help-files/introduction/summary_measure_details_global_warming_potential.html. (Accessed 8 November 2021).

[60] E. Silla, A. Arnau, I. TuñóN, Fundamental principles governing solvents use, Handbook of Solvents (2001) 7.

[61] J.D. Silvestre, Life Cycle Assessment 'from Cradle to Cradle' of Building Assemblies—Application to External Walls, Instituto Superior Técnico, Lisbon, Portugal, 2012. Ph.D. Thesis.

[62] Y. Bicer, I. Dincer, Life cycle environmental impact assessments and comparisons of alternative fuels for clean vehicles, Resour. Conserv. Recycl. 132 (2018) 141–157, https://doi.org/10.1016/j.resconrec.2018.01.036.

[63] R. Kurda, Sustainable Development of Cement-Based Materials: Application to Recycled Aggregates Concrete, Doctoral dissertation, Instituto Superior Técnico, Universidade de Lisboa, 2017.
[64] J.B. Guinée, Handbook on Life Cycle Assessment: Operational Guide to the ISO Standards, 7, Springer Science & Business Media, 2002.
[65] J. Bare, D. Young, S. Qam, M. Hopton, S. Chief, Tool for the Reduction and Assessment of Chemical and Other Environmental Impacts (TRACI), US Environmental Protection Agency, Washington, DC, USA, 2012.
[66] European Commission, Product Environmental Footprint Category Rules Guidance, 2018.
[67] J.C. Knudson, G.B. Crane, R.S. Briggs, Atmospheric Emissions from Chlor-Alkali Manufacture, Environmental Protection Agency, Air Pollution Control Office, 1971.
[68] L. Imtiaz, S. Kashif-ur-Rehman, W.S. Alaloul, K. Nazir, M.F. Javed, F. Aslam, M.A. Musarat, Life cycle impact assessment of recycled aggregate concrete, geopolymer concrete, and recycled aggregate-based geopolymer concrete, Sustainability 13 (24) (2021), 13515, https://doi.org/10.3390/su132413515.
[69] J. Hou, P. Zhang, X. Yuan, Y. Zheng, Life cycle assessment of biodiesel from soybean, jatropha and microalgae in China conditions, Renewable Sustainable Energy Rev. 15 (9) (2011) 5081–5091, https://doi.org/10.1016/j.rser.2011.07.048.
[70] V. Li, Development of Green ECC for Sustainable Infrastructure Systems Multi-Physics and Multi-Scale Modelling of Next Generation Sustainable Civil Infrastructure View Project Concrete Materials; Engineering Cementious Composites View Project Development of Green Ecc for Sustainable Infrastructure Systems, 2004.